A Guide to WSR-88D Data Quality Phenomena and Anomalies

Radar Support Team
Operations Branch
Radar Operations Center
Norman, OK 73069
August 2024

Throughout the operational life of the WSR-88D numerous phenomena and items of interest have been observed in WSR-88D data from wedges of erroneous Differential Reflectivity (ZDR) data and radial spikes to elevation discontinuities and reflections. Many of these provide erroneous information that can cause confusion among forecasters and operators. While some are the result of software bugs which can be mitigated in future software changes (and are available in the **Past Topics** section), the majority of these phenomena are products of nature, physical constraints of the system, or failure of specific hardware components and, thus, have the potential of being present in the data given the right set of circumstances. In this paper, a broad collection of these anomalies are presented with discussion on the impact to the users of the data.

A list of **acronyms** is available on the last page.

Current Topics:

Biological Targets

It is rather common, especially in the warm season, to see numerous biological targets (i.e., insects, birds, and even vegetation) on radar displays. These radar returns can be quite strong, exceeding 30, sometimes 40 dBZ. In addition to relatively high R values, ZDR values will often also be high while CC values will be low. The addition of Dual Pol variables allows us to confirm that the strong R returns are non-meteorological.

A video at http://www.npr.org/sections/krulwich/2011/06/01/128389587/look-up-the-billion-bug-highway-you-cant-see discusses just how many insects can be within a 0.6-mile column of air.

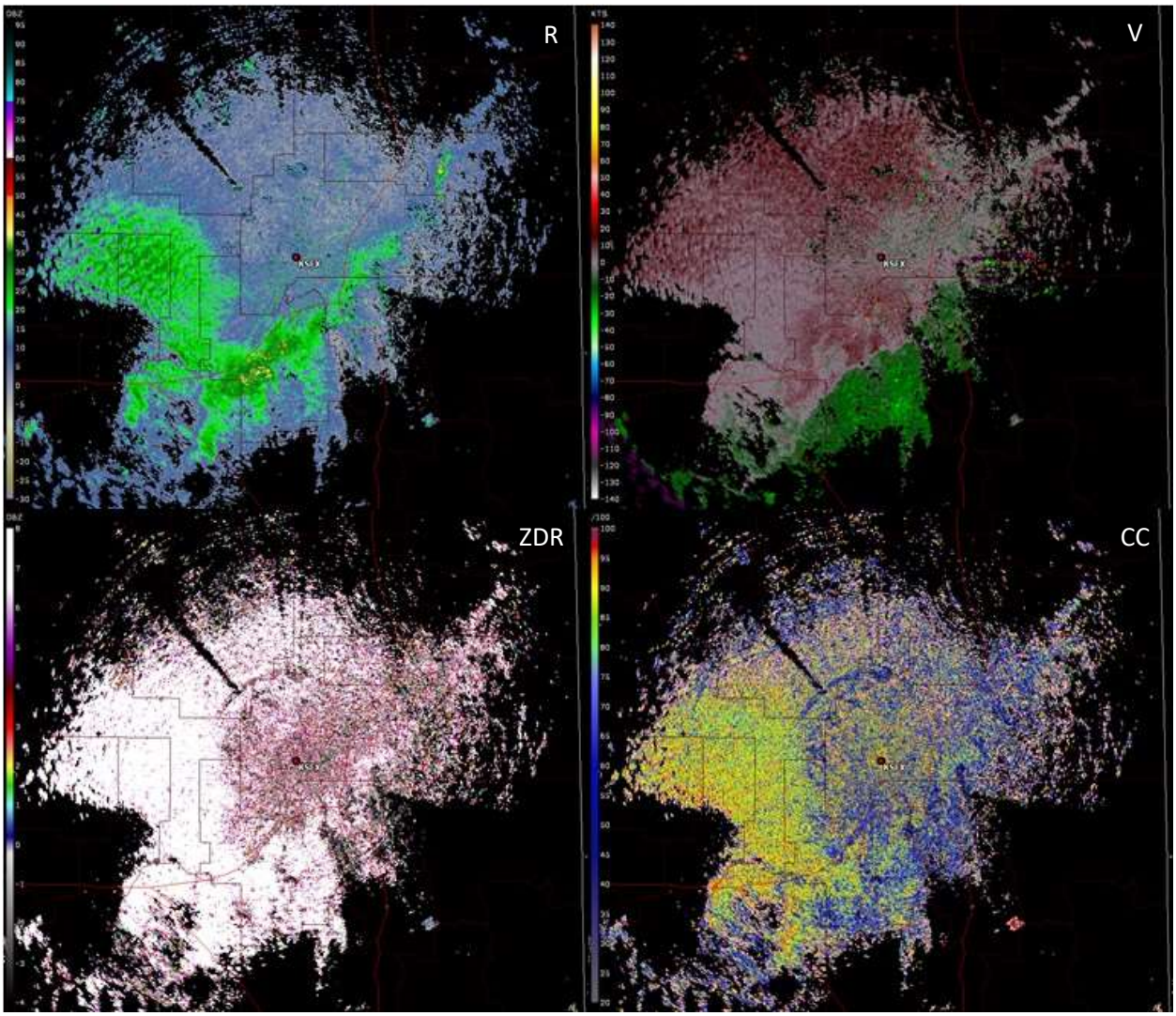

Bird & Bat Signatures

Other examples of WSR-88Ds detecting biological targets include birds and bats departing roosts and caves. Birds are often seen flying away from their nesting grounds near sunrise while bats are seen flying away from their caves near sunset. The radar returns often start out in a circular appearance, then gradually disperse as the animals change their course. They often show divergent velocity signatures, and Dual-Pol variables add to the confirmation that these returns are biological. CC and ZDR estimates are influenced by the orientation of the biological targets with respect to the beam. For more discussion related to the impact of the shape of the biological targets on the scattering of the beam as well as interpretation of WSR-88D products refer to https://esajournals.onlinelibrary.wiley.com/doi/10.1002/ecs2.1539.

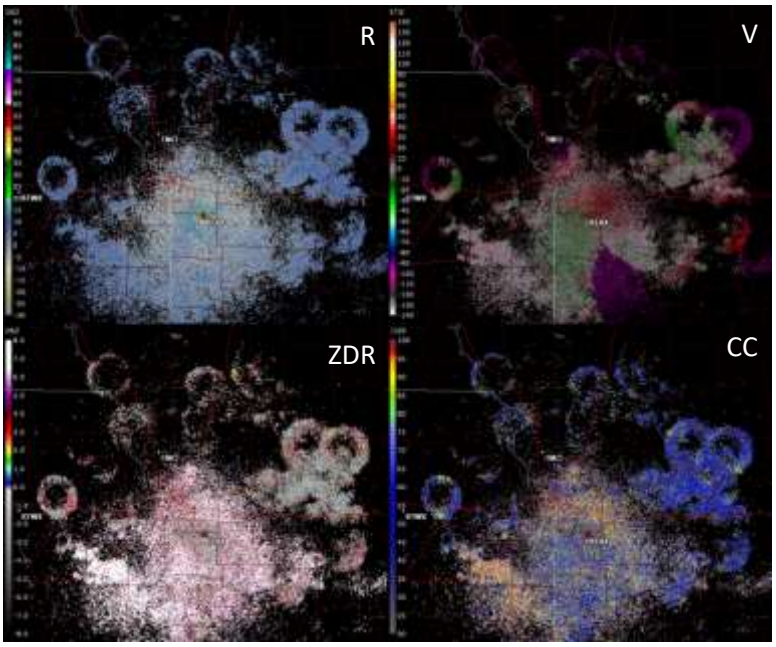

Bird signatures over northern and central Missouri and eastern Kansas during clear air.

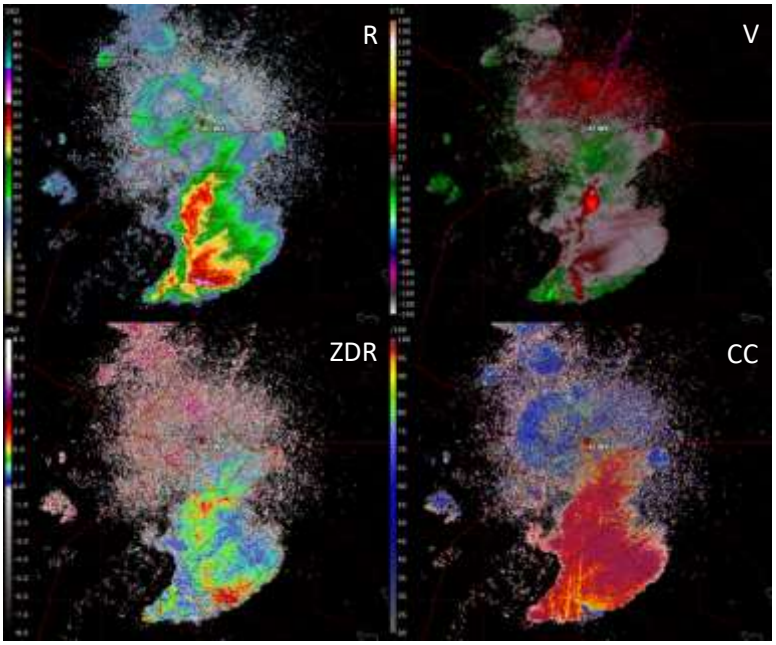

Bat signatures near San Antonio, Texas during severe storms.

Bistatic Coupling

Two rotating pulsed radars (e.g., Doppler) operating with similar frequencies can interfere with each other resulting in interference known as Bistatic Coupling, which is sometimes referred to as “Running Rabbits”. Typically this phenomenon occurs when the two radars sample the same target (e.g., thunderstorm) at the same time and altitude. Common clusters of WSR-88Ds are located in the Central U.S., Southeast U.S., and Northeast Corridor. See page 7 of this NEXRAD Now article for more information on Bistatic Coupling.

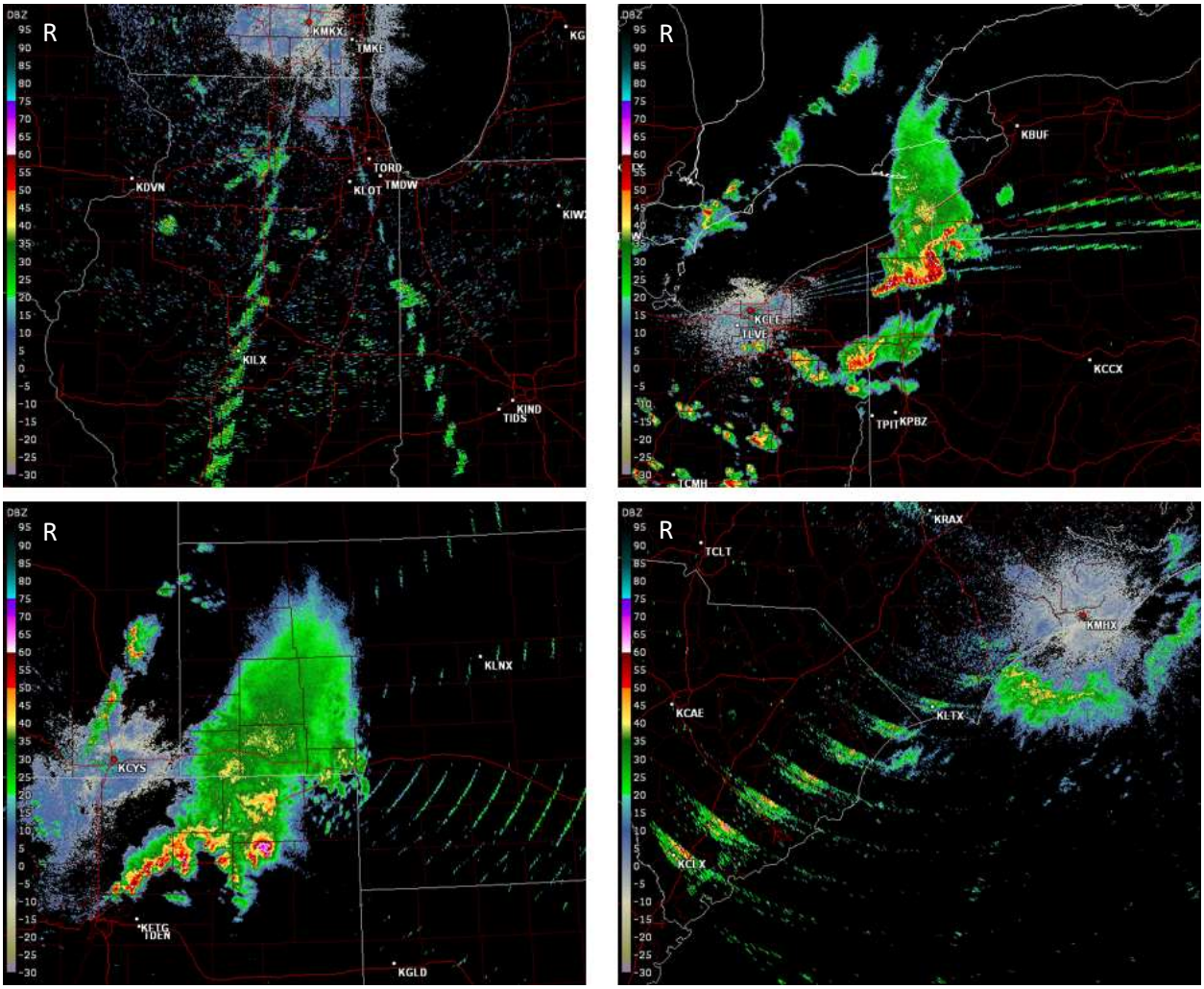

Chaff

Chaff is strips of metal foil dropped by military aircraft as a radar countermeasure and can be observed on radar products. The images below contain chaff and precipitation. Chaff has been observed since before the Dual-Pol upgrade; however, discrimination between chaff and precipitation echoes was eased due to the upgrade. Typically, radar returns from chaff have low CC and high ZDR values.

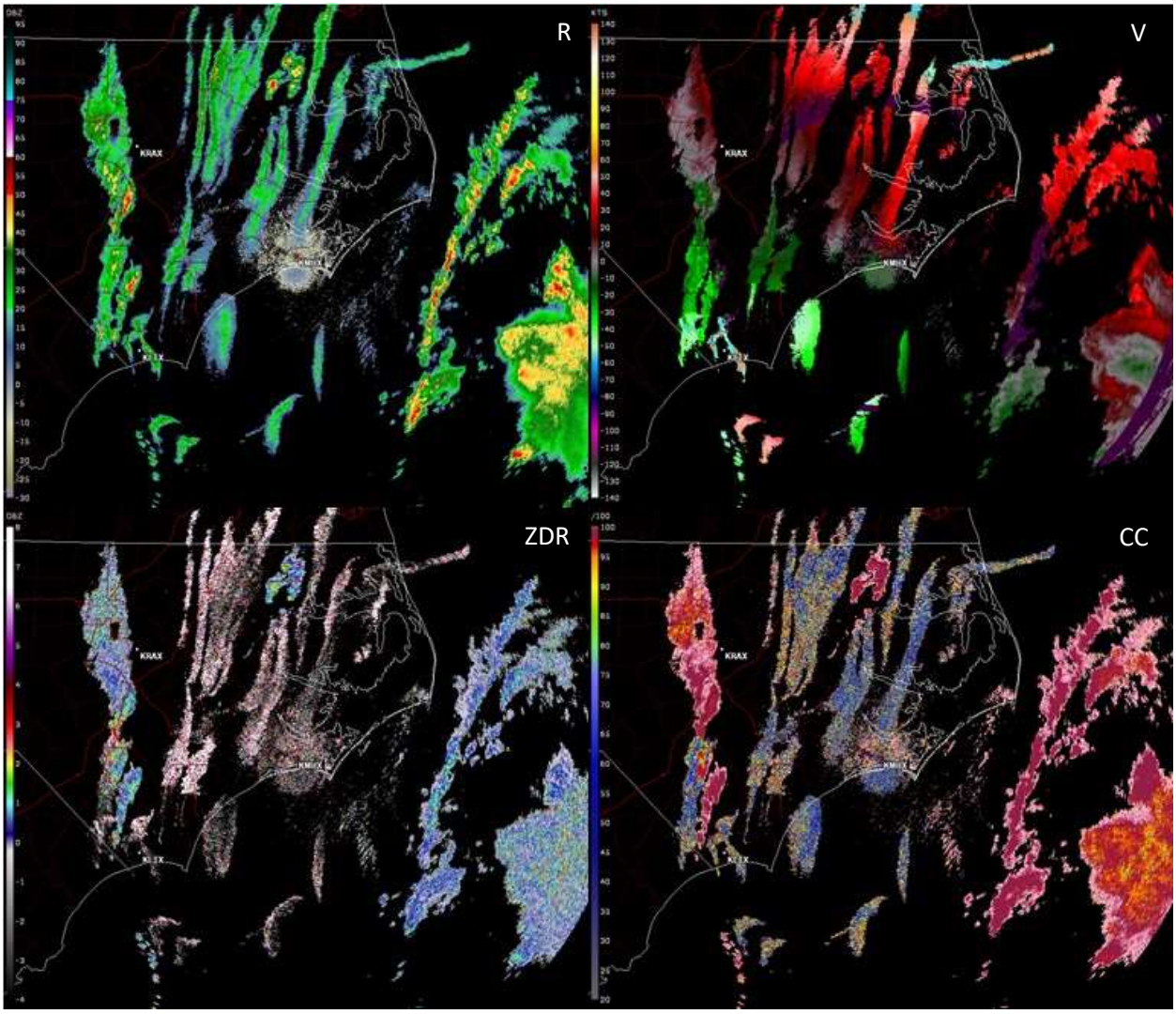

CMD False Alarms

False alarms can occur with the current version of CMD, but the number of false alarms on Split Cuts has been reduced following improvements to the algorithm. False alarms can be quite noticeable on Batch Cuts, depending on the meteorological conditions. While we are referring to these as CMD false alarms, the underlying issue is with the Bypass Map as described in the "Data Voids from Bypass Map" issue in this document. The example below is from 1.8 degrees, which is a Batch Cut.

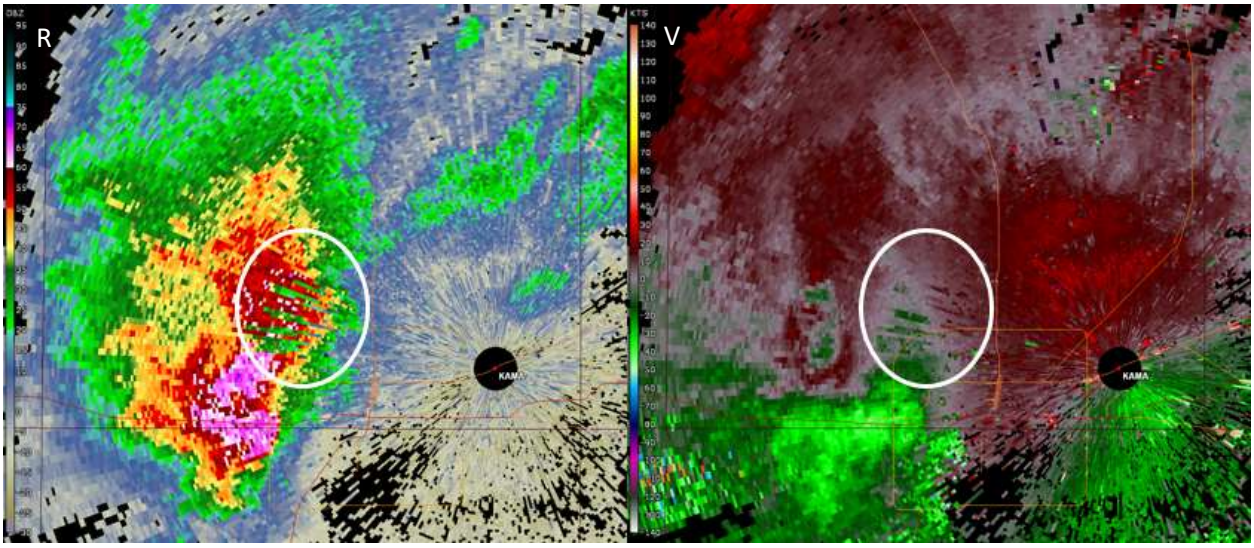

Data Voids from Bypass Map

During the first implementation of CMD, numerous field sites noticed box-shaped areas of reduced reflectivity (i.e., data voids), mainly along the zero isodop but also in areas where velocity values are a multiple of the Nyquist Interval of the Surveillance Split Cut scan. In troubleshooting, it was found that these voids have existed since pre-ORDA and are a result of the creation of the clutter bypass map. Prior to the deployment of CMD, these voids were static or stationary, which eventually became disregarded. With CMD, these data voids move from one volume to the next, depending on the bins that were flagged as containing clutter by the algorithm, catching the eye with their movement.

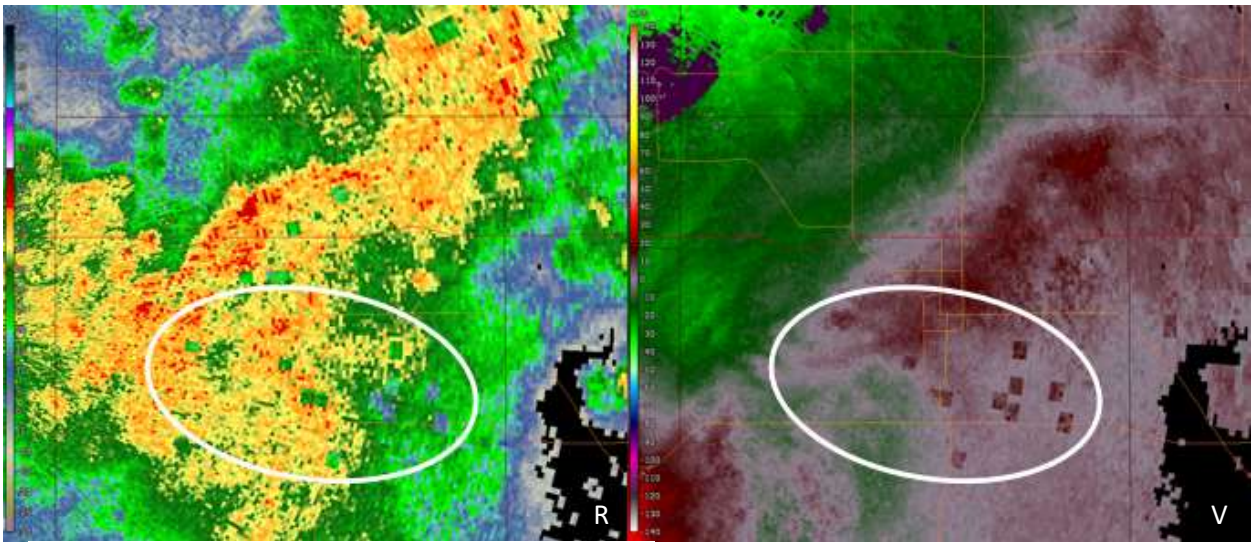

Example of reflectivity data voids along zero isodop.

Due to the way GMAP filters data, the velocity data in these areas are biased away from zero.

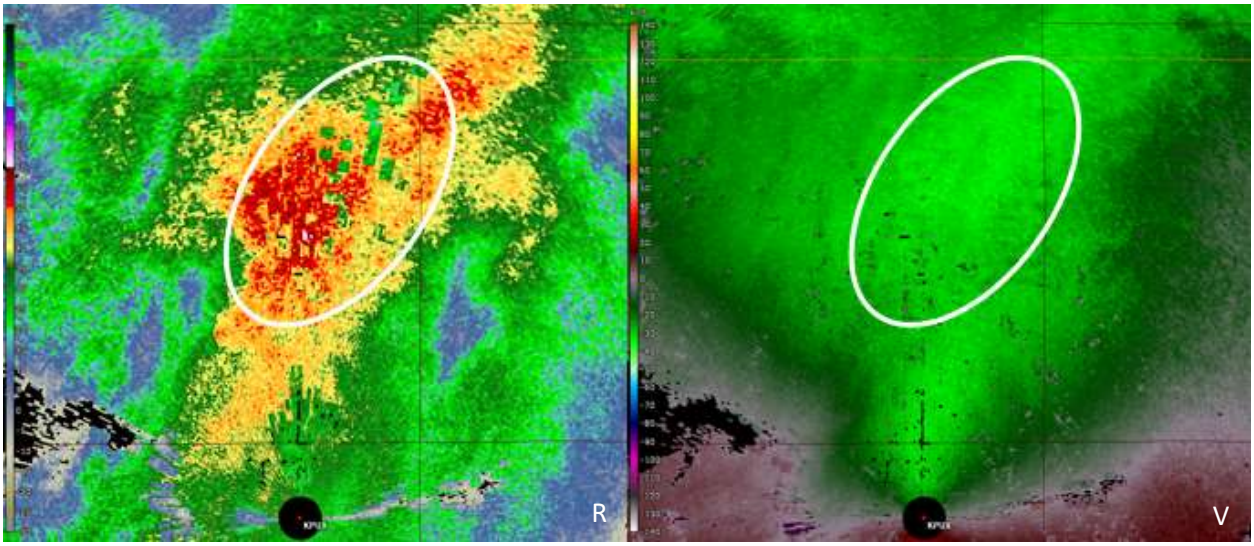

Example of reflectivity data voids for a multiple of the Nyquist.

In these cases, the impacts to velocity data are negligible.

Earthquakes

Biologicals often take flight immediately following an earthquake in their vicinity. A 4.3 earthquake occurred near Edmond, OK at 11:39 UTC on 29 December 2015 causing thousands of biologicals to take flight. The images below illustrate this phenomenon where the yellow star shows the location of the epicenter.

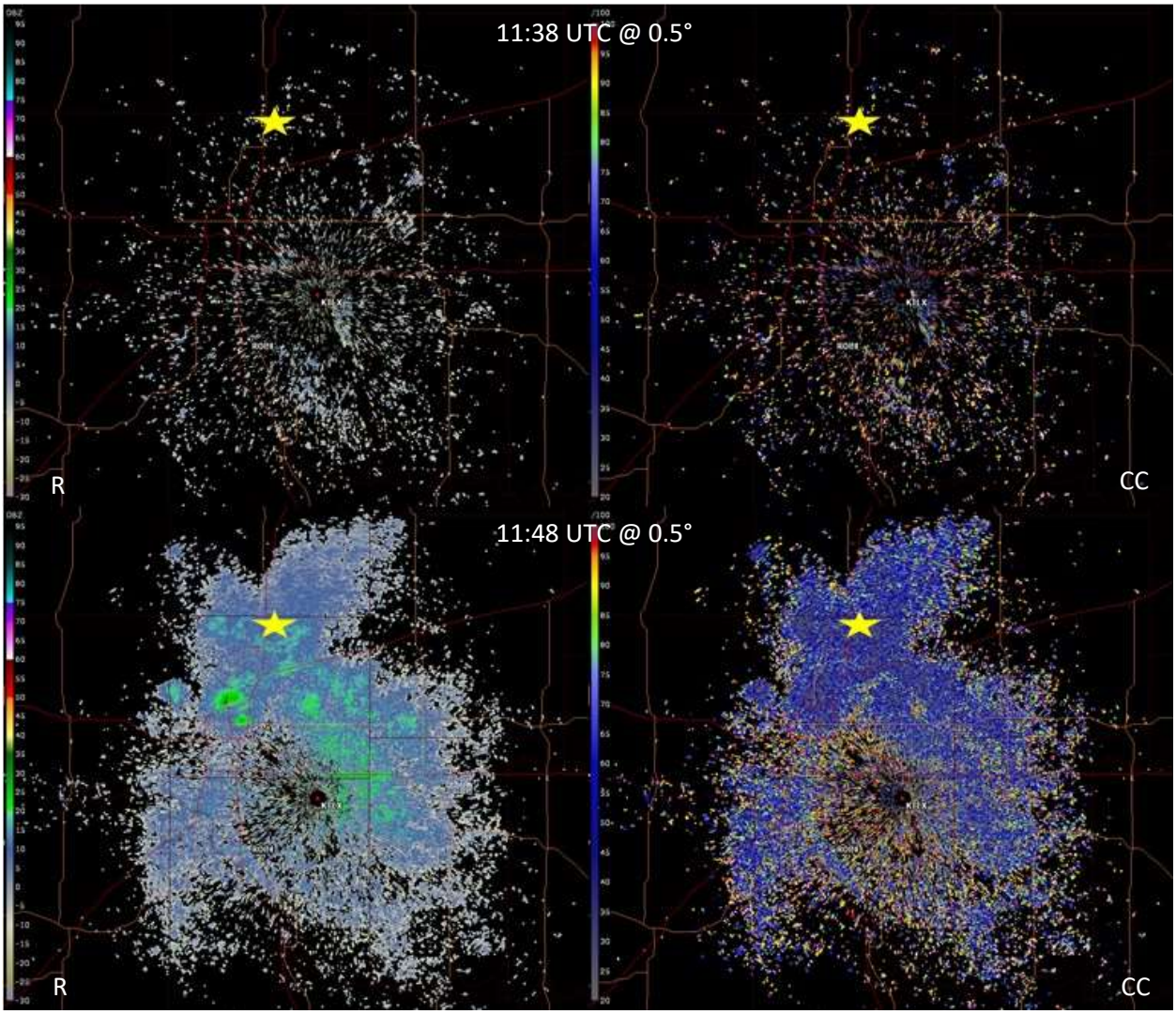

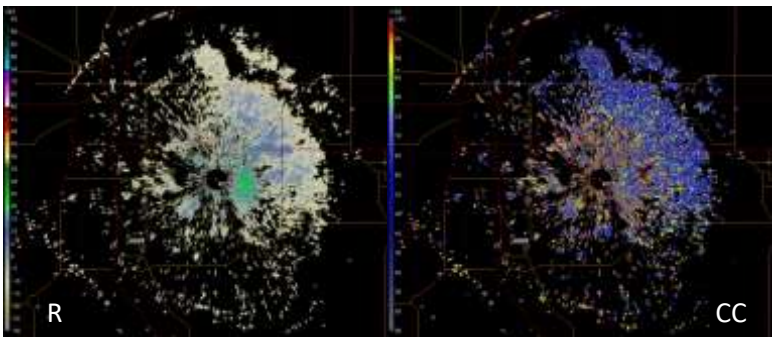

The images to the left are from 1.5°, two minutes after the earthquake.

Exclusion Zone Holes

The hybrid scan requires that the rainfall rate grid achieve a minimum percentage to be considered filled (or full). For both the PPS and QPE, this percentage is 99.9. The percentage is checked at the end of each cut. Once that percentage is reached, the hybrid scan is complete and the data (i.e., hybrid reflectivity for PPS; hybrid hydrometeor class for QPE) are sent downstream in the algorithm to be converted to rainfall estimates. If the percentage is reached before the maximum elevation angle of an exclusion zone is reached then a "no data" wedge can result.

Sites experiencing this can minimize the size of the exclusion zone, in azimuth, range, and elevation. The purpose of exclusion zones is to remove clutter—some of which may have motion—from the precipitation accumulations. Note: Exclusion zones do NOT impact base data. Exclusion zones may also be used to mitigate stationary ground clutter not always completely removed my GMAP.

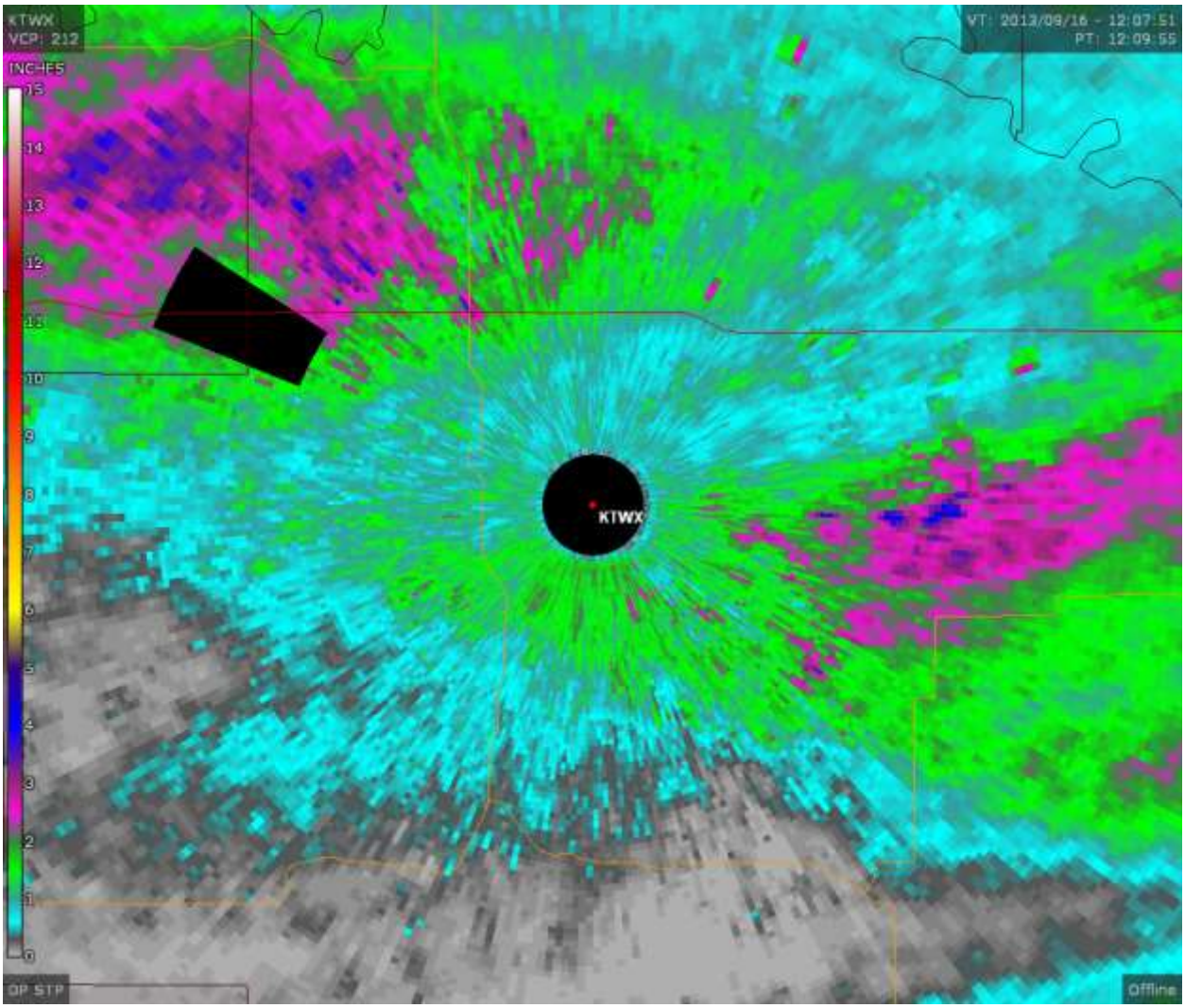

External Interference

Interference is a rather common observation in WSR-88D data and has different appearances depending on the interfering source. A few examples of sources include cell phone towers, aircraft, and other radar systems. Some WSR-88Ds may only observe interference during beam ducting conditions or inversions while other WSR-88Ds may observe interference more consistently. Data images of some interference signatures follow.

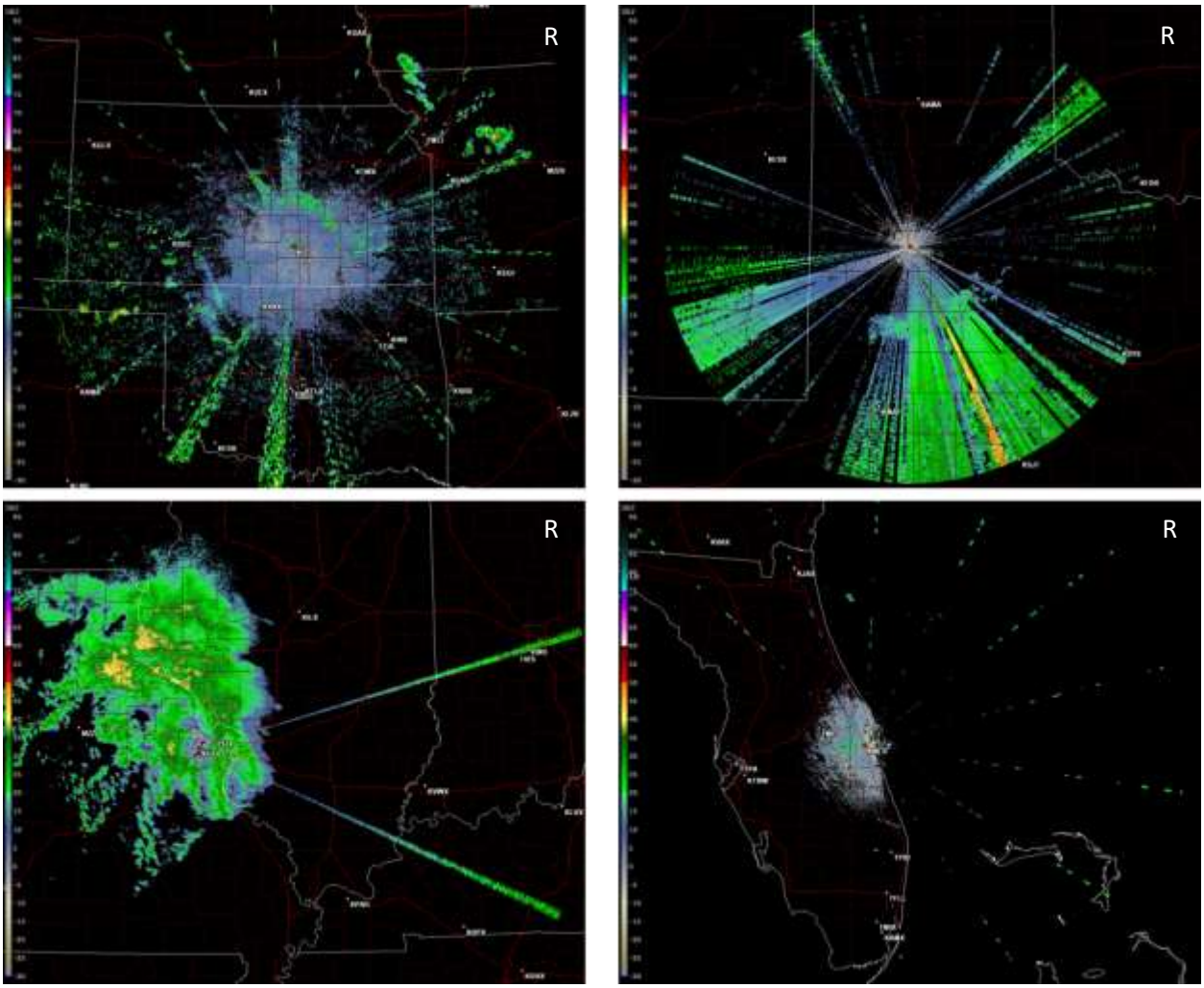

Non-Uniform Beam Filling

The phenomenon known as Non-Uniform Beam Filling (NBF) occurs when there is a sharp gradient of PHI within the beam resulting in reductions in CC down radial. NBF can often be observed during squall lines aligned along a radial or thunderstorms with sufficiently strong cores near the melting layer height. If CC drops below 0.9 then the radar echo is considered to be non-meteorological, which can lead to algorithm errors where CC is an input.

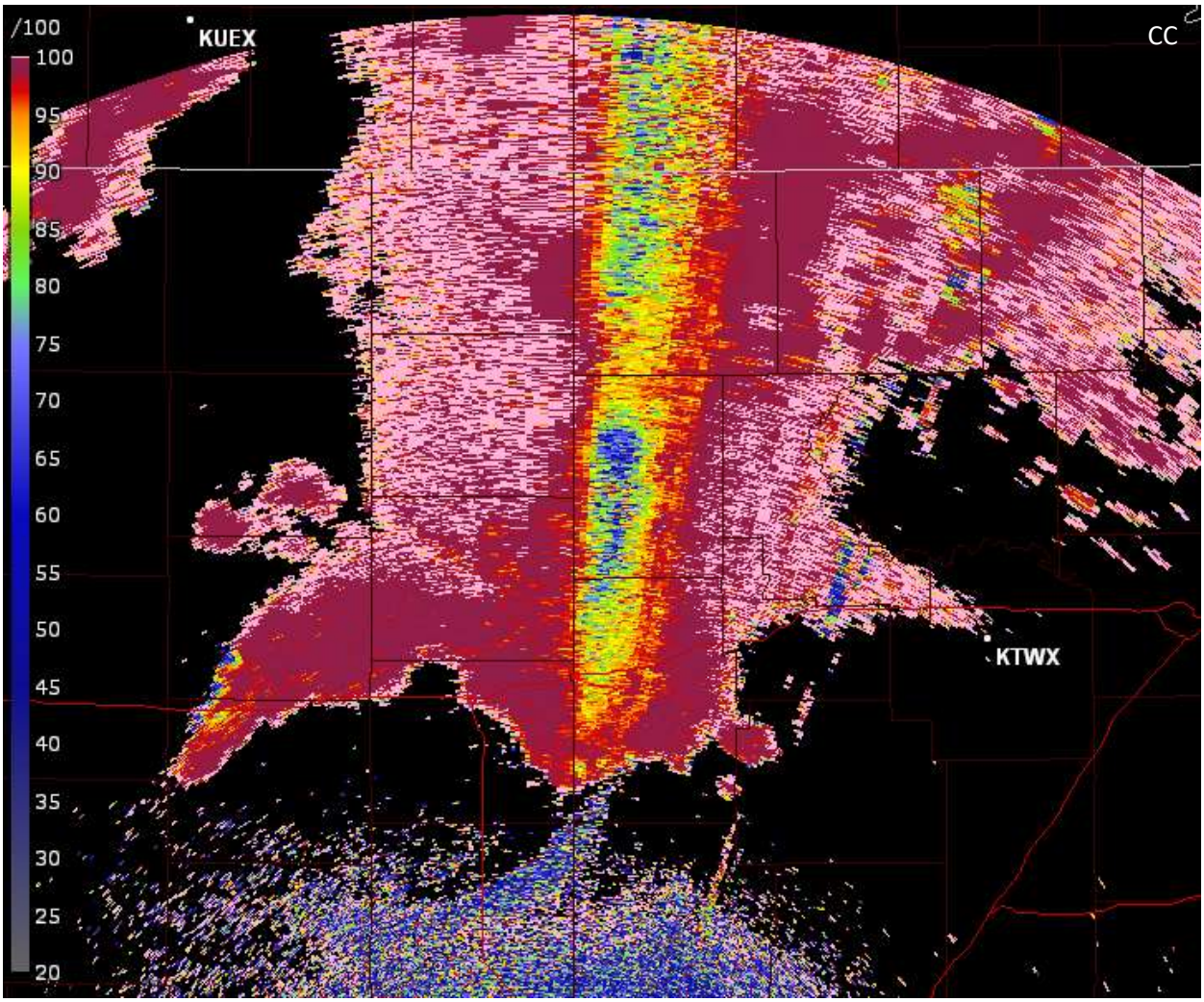

PHI Wrapping

When the initial PHI data are close to zero (i.e., 350-10 degrees), the RPG cannot properly process the data due to wrapping. Wrapping PHI data negatively impacts several Level 3 products, including ZDR, KDP, HC/HHC, and QPE. The problem can be resolved by manually updating the ISDP Adaptation Data value (i.e., st22) or accomplishing the ISDP calibration routine during appropriate conditions (i.e., light rain from 5 to 30 km from the radar). The PHI data can be evaluated in a Level 2 data viewer or in AWIPS via the raw PHI product. High PHI values have a big impact on the downstream products resulting in very high Level 3 ZDR estimates, a spoke-like appearance in KDP, erroneous HCA classifications, and low Dual-Pol precipitation estimates. In this case, the ZDR estimates in Level 2 data versus Level 3 data will often look very different, with Level 3 estimates appearing high as compared to the Level 2 estimates. Note: High Level 3 ZDR estimates do not necessarily mean an ISDP issue. Verification of Level 2 data is required. Contact the WSR-88D Hotline for assistance.

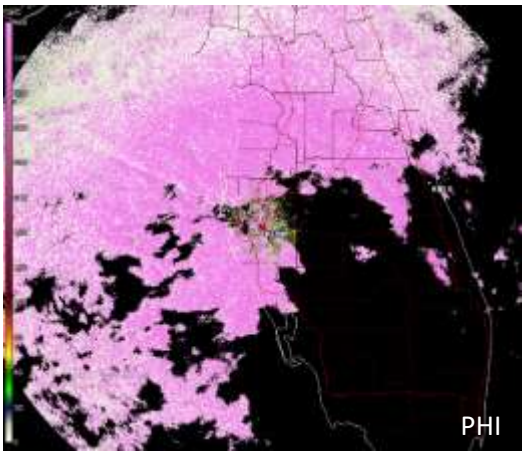

These two images illustrate PHI wrapping. The image on the left displays very high PHI values while the image on the right shows very low PHI values.

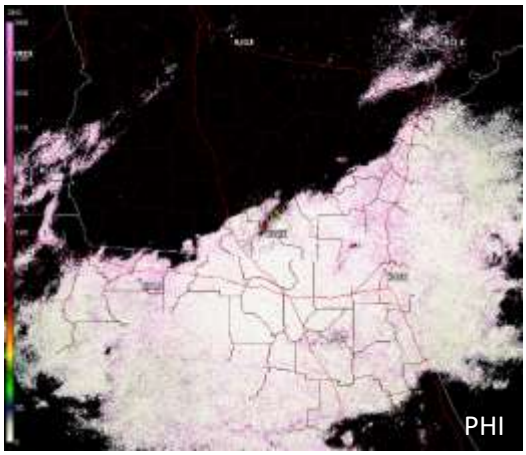

The image below illustrates the impact of high PHI values on the Level 3 ZDR.

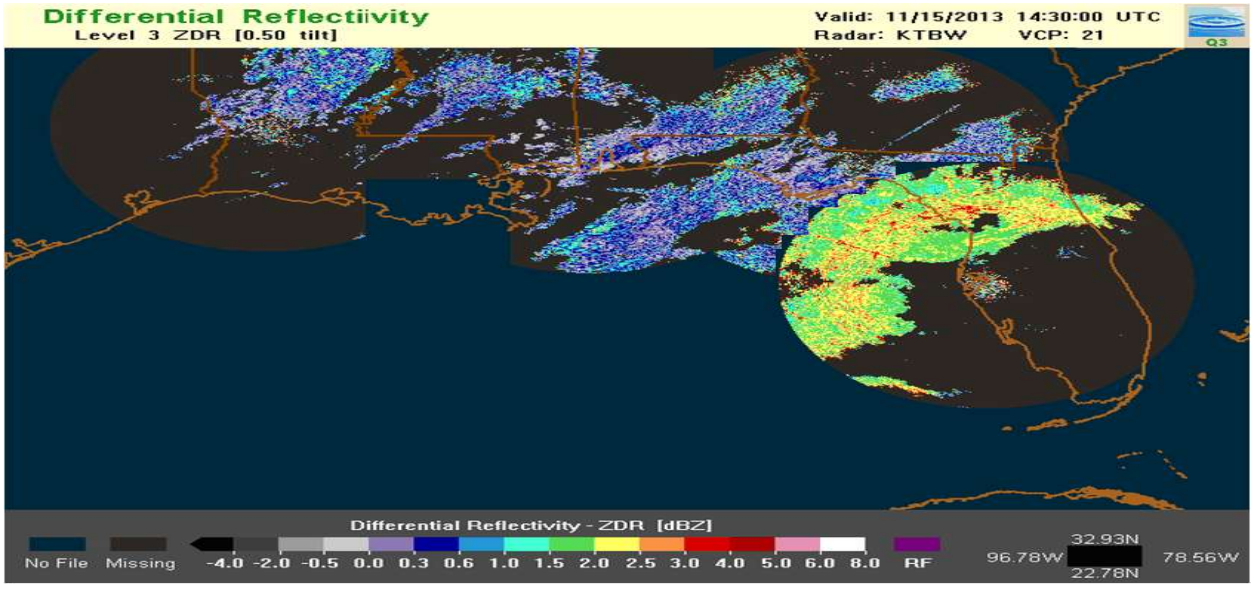

Pointing Errors

Though typically rare, pointing errors can occur. These errors can happen in elevation or azimuth following certain maintenance activities. Comparing data from multiple adjacent radars can aid in determining if a pointing error exists. Errors can vary in magnitude. Contact the WSR-88D Hotline for assistance if a pointing error is suspected.

The 0.5-degree R images of the elevation pointing error example below are just about an hour apart. Note how the clear air bloom is much smaller in the image on the right. Further investigation of upper elevations revealed that despite a reported angle of 0.5 degrees, the radar was scanning closer to 1.3 degrees as suggested by the standard appearance/coverage of the clear bloom prior to the error.

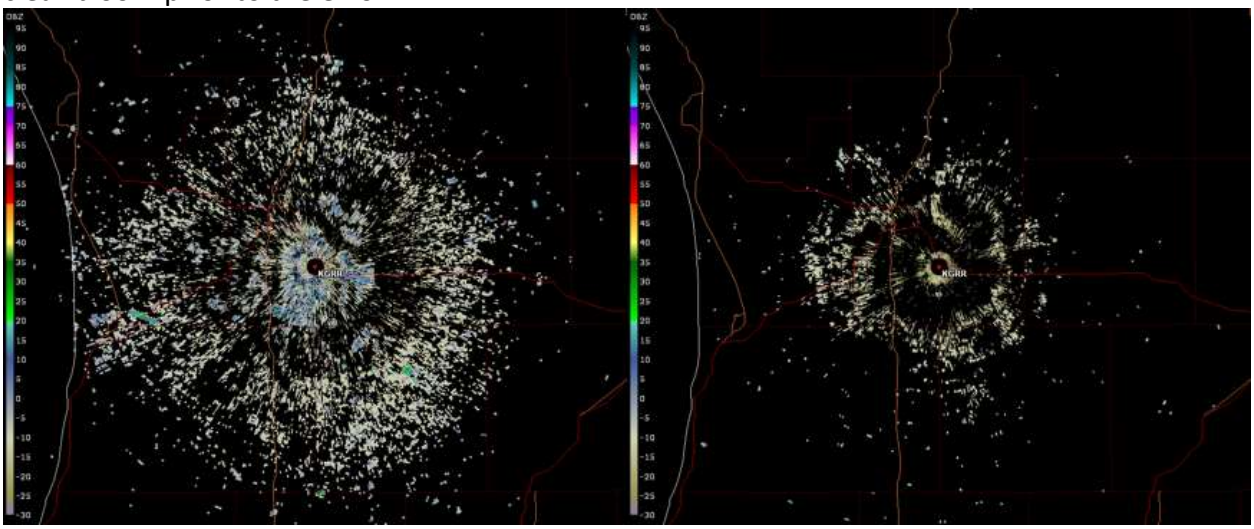

In the example below, two radars were displaying the precipitation shield in very different locations. The radar on the right was displaying the precipitation about 90 degrees clockwise of its true location. Large azimuth pointing errors are rather straightforward to spot; small azimuth errors require many comparisons in which known clutter targets can provide insight to the magnitude of the error.

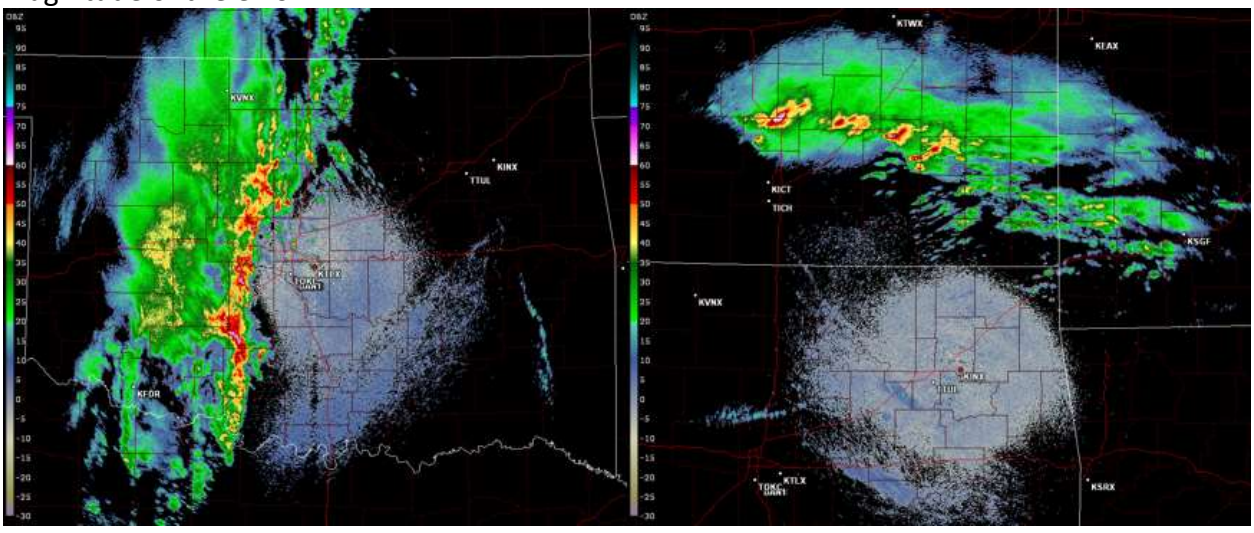

Popcorn Cities

During certain conditions, mainly occurring during the warm season, cities and towns near WSR-88D sites can be observed on the display as they “pop” up on radar. Termed “popcorn cities”, these towns show up as a cluster of returns, likely due to the heat island effect.

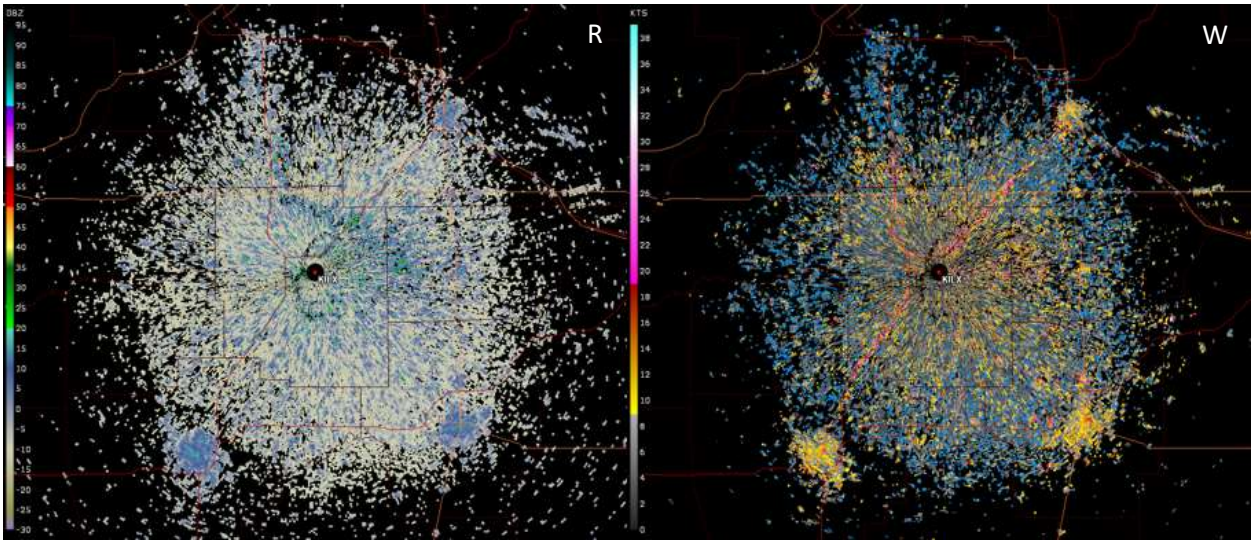

QPE Rings/Discontinuities

Discontinuity rings may be present in QPE accumulation products. These discontinuities can be collocated with the top or the bottom of the melting layer depending on the cause. Hydrometeor classifications assigned above the top of the melting layer are dry snow (DS) and ice crystals (IC). The rain rate relationship used for these classifications is M*R(Z), where M is some multiplier between the values of 1.0 and 2.8 and is chosen by the radar operator. The default value is 2.8 degrees, which often results in abnormally high precipitation estimates. Several rings may be observed in accumulations due to the change in the height of the melting layer throughout an event. A field test was conducted among sites in Eastern Region in order to determine a more appropriate multiplier for each participating site. These values ranged from 1.5 to 1.9 and significantly reduced the discontinuity at the top of the melting layer. Below are two images of the QPE DSA from the same precipitation event. In the image on the left, M was set to 2.8 for both DS and IC. In the image on the right, M was set to 1.5 for these hydrometeors.

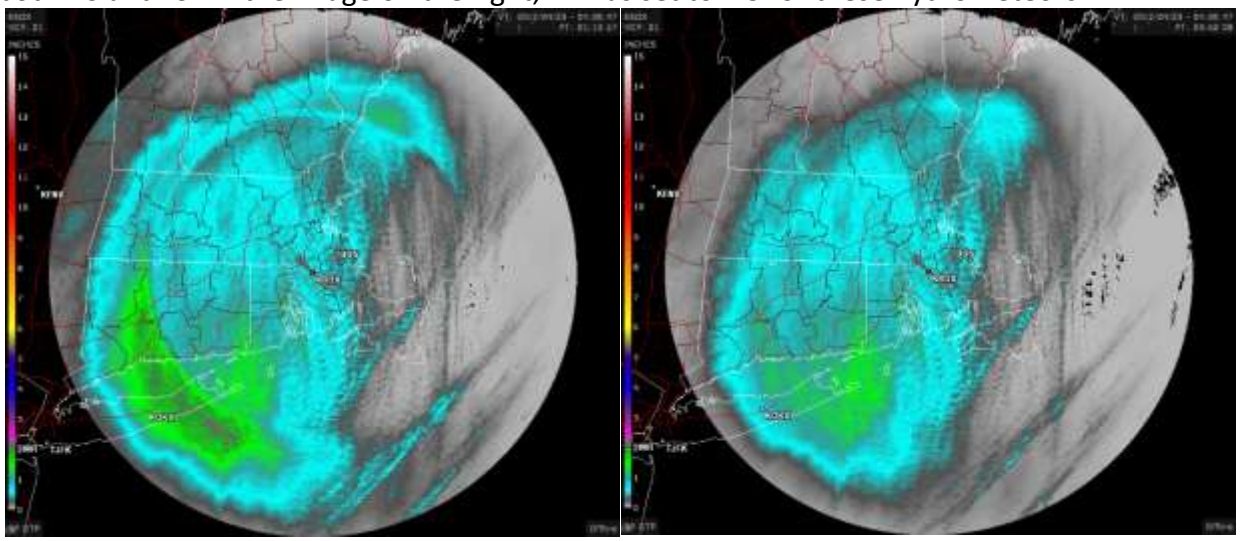

A ring in QPE can also be present near the bottom of the melting layer due to the use of Specific Attenuation, R(A). This rain rate relationship is used by QPE only below the melting layer (i.e., liquid targets).

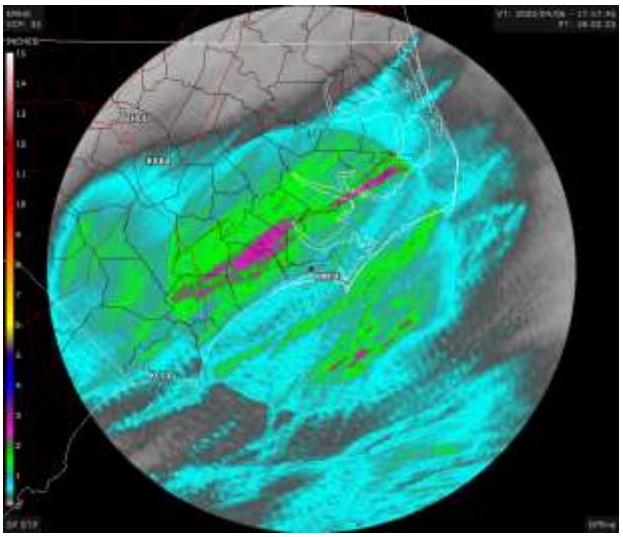

Reflections

It is not uncommon to observe reflections from echoes on the display. Reflections can occur when the radar beam hits a large clutter target (i.e., blockage), usually in close proximity to the radar. Pulses from the beam can bounce—or reflect—off of the clutter target, sending them in a new direction perpendicular to the reflector. When the reflected pulses return to the radar, the radar remembers the azimuth in which they were originally sent and paints any intercepted echoes along that radial resulting in an apparent spike. This phenomenon may be easily observed when the reflected pulses intercept precipitation—in this case the characteristics of the spike will be similar to that of precipitation, and the spike will appear to move at the rate of the approaching precipitation. Once the reflected pulses do not encounter any echoes, then the spike will no longer be visible.

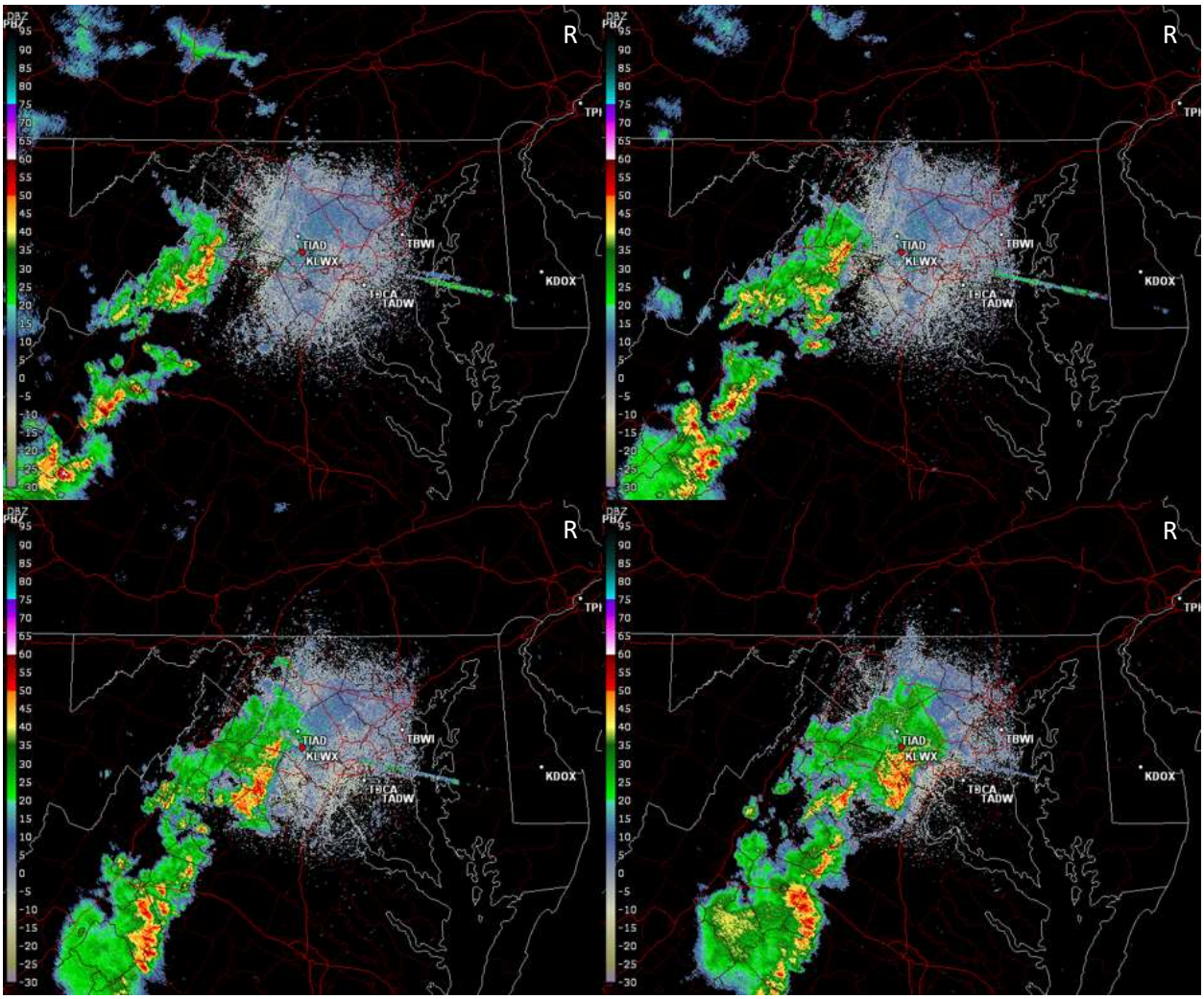

Reflections, continued

As the precipitation progresses and crosses over the radar, the radial once showing a reflection may show a blockage. This is because the reflector often is a blockage, or partial blockage, as illustrated in the example below. In the image on the left, a reflection can be observed to the southeast. Once the precipitation moves over that radial a void can be seen indicating a blockage along the radial.

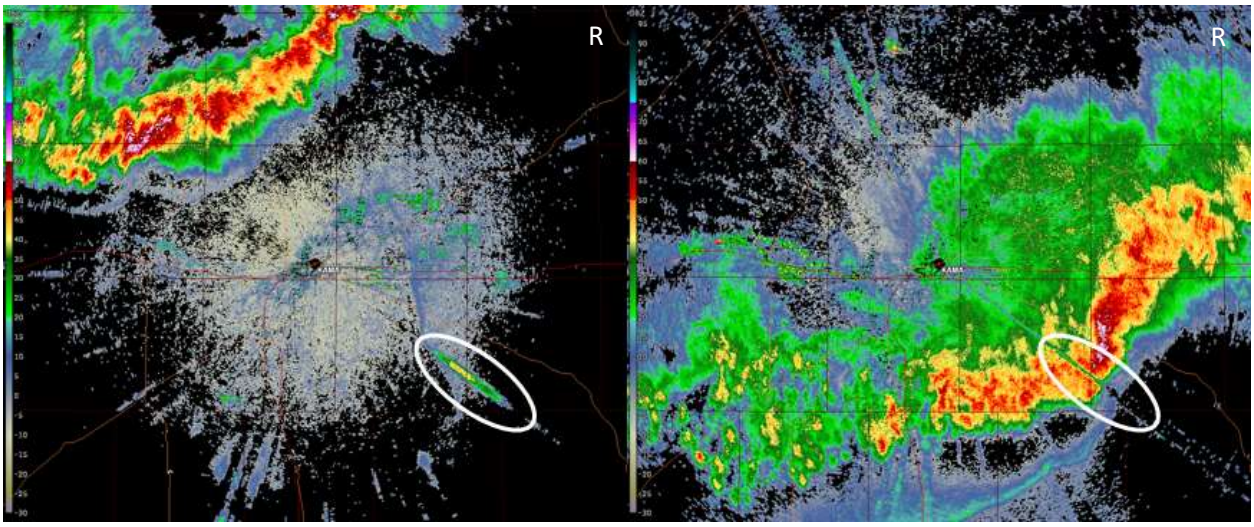

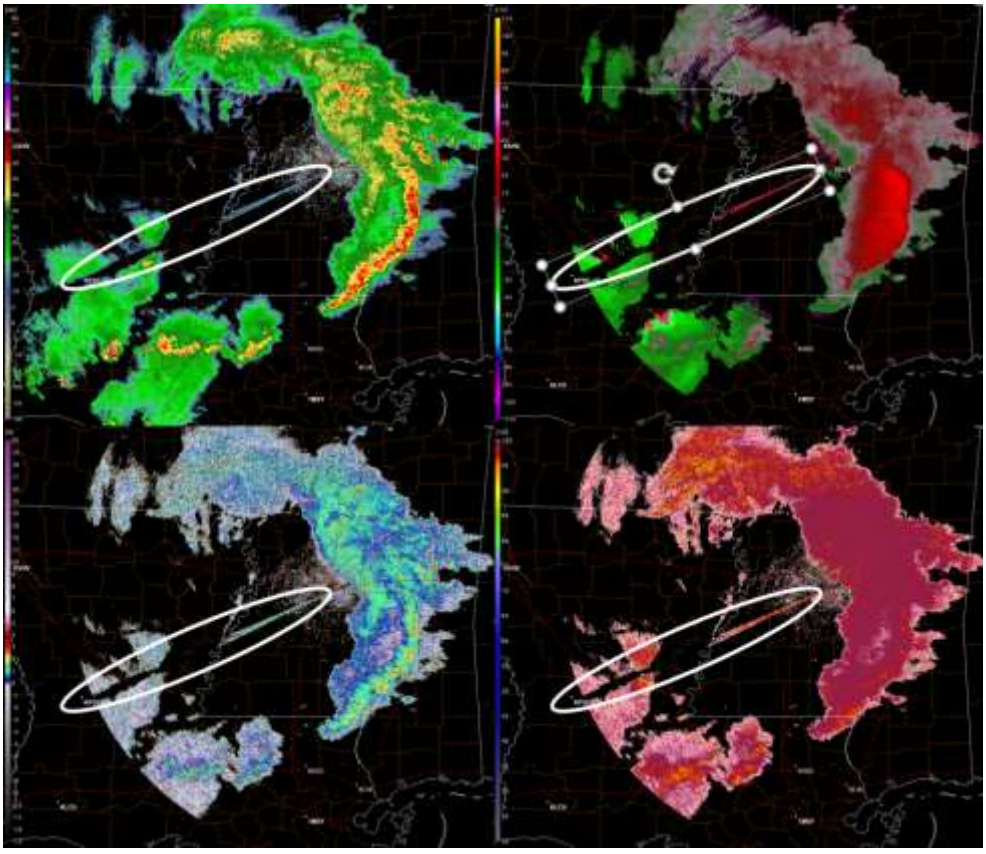

The images to the left show a blockage and its reflection at the same time. This can occur when there is sufficient echo both within the radial of the blockage as well as in the radial perpendicular to the reflector.

As mentioned on the previous page, the reflection has characteristics similar to those of the precipitation.

Second Trip Echoes

One somewhat rare phenomenon is second trip echo. These are rare due to the combination of ingredients needed for them to occur. First, there needs to be significant beam ducting occurring and there needs to be a strong echo present at far range (i.e., greater than 251 nmi, which is the maximum unambiguous range of the lowest Contiguous Surveillance cut for WSR-88Ds VCPs) this is visible by the radar experiencing beam ducting.

In the example below, the three leftmost images depict a second trip echo observed by the Topeka, KS (KTWX) radar. Note that the ZDR and CC suggest the echo is meteorological. In these images, evidence of beam ducting can be observed towards the northeast. The rightmost image shows strong thunderstorms near the Davenport, IA (KDVN) radar. The near-edge of these storms is roughly 265 nmi from KTWX, 14 nmi beyond the maximum unambiguous range of the PRF being used. By the time KTWX received the returned pulse that sampled the storm near KDVN, another pulse had been transmitted. It thinks the returned signal is from a different pulse and displays the signal at the corresponding range of the subsequent pulse; in this case at about 14 nmi.

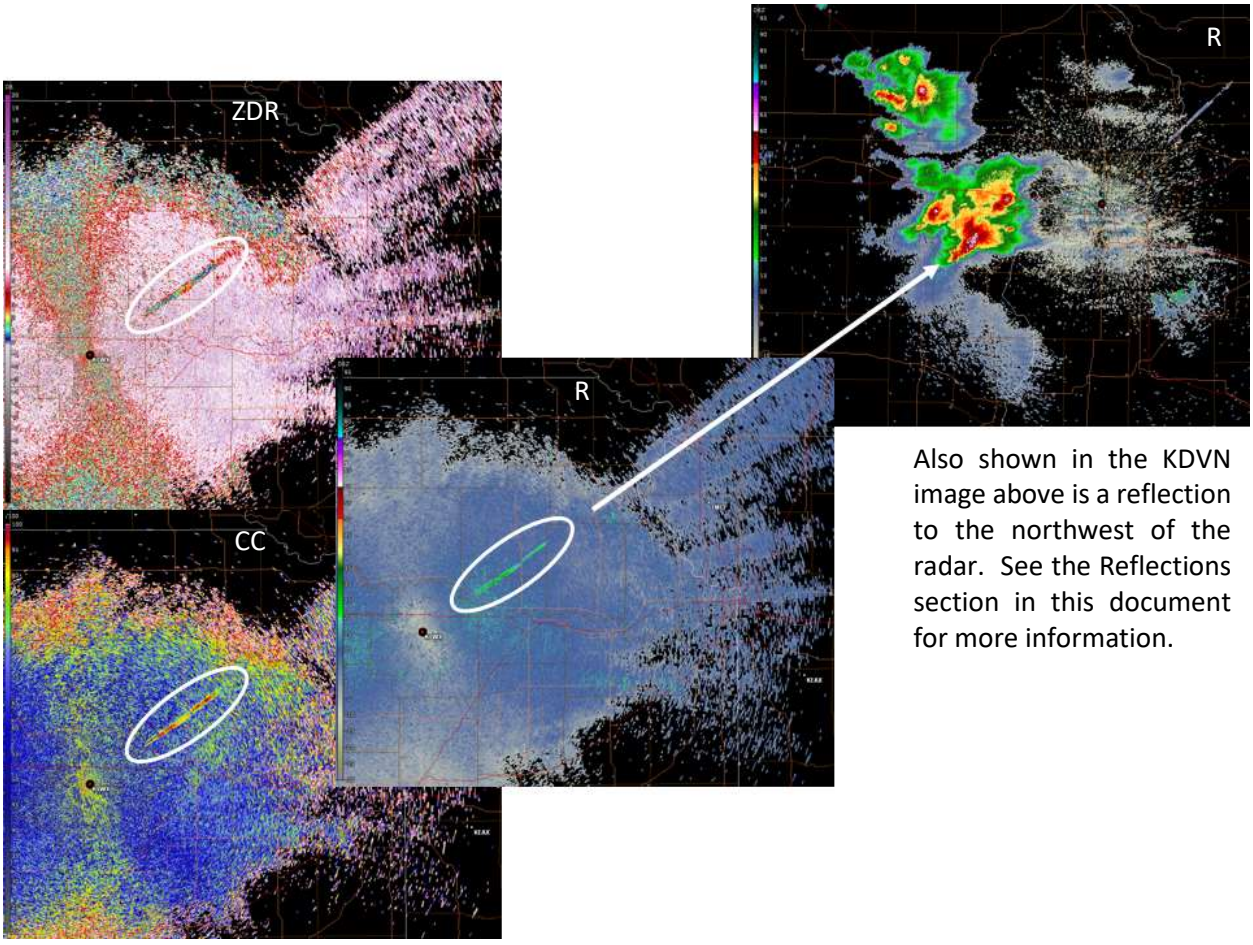

Also shown in the KDVN image above is a reflection to the northwest of the radar. See the Reflections section in this document for more information.

Sea Spray

Observation of sea spray is rather common on low-elevation angles from WSR-88Ds near large sources of water. The low CC values and low ZDR values indicate that the returns are from non-precipitating echoes. Evaluating R and V alone does not necessarily draw the same conclusion.

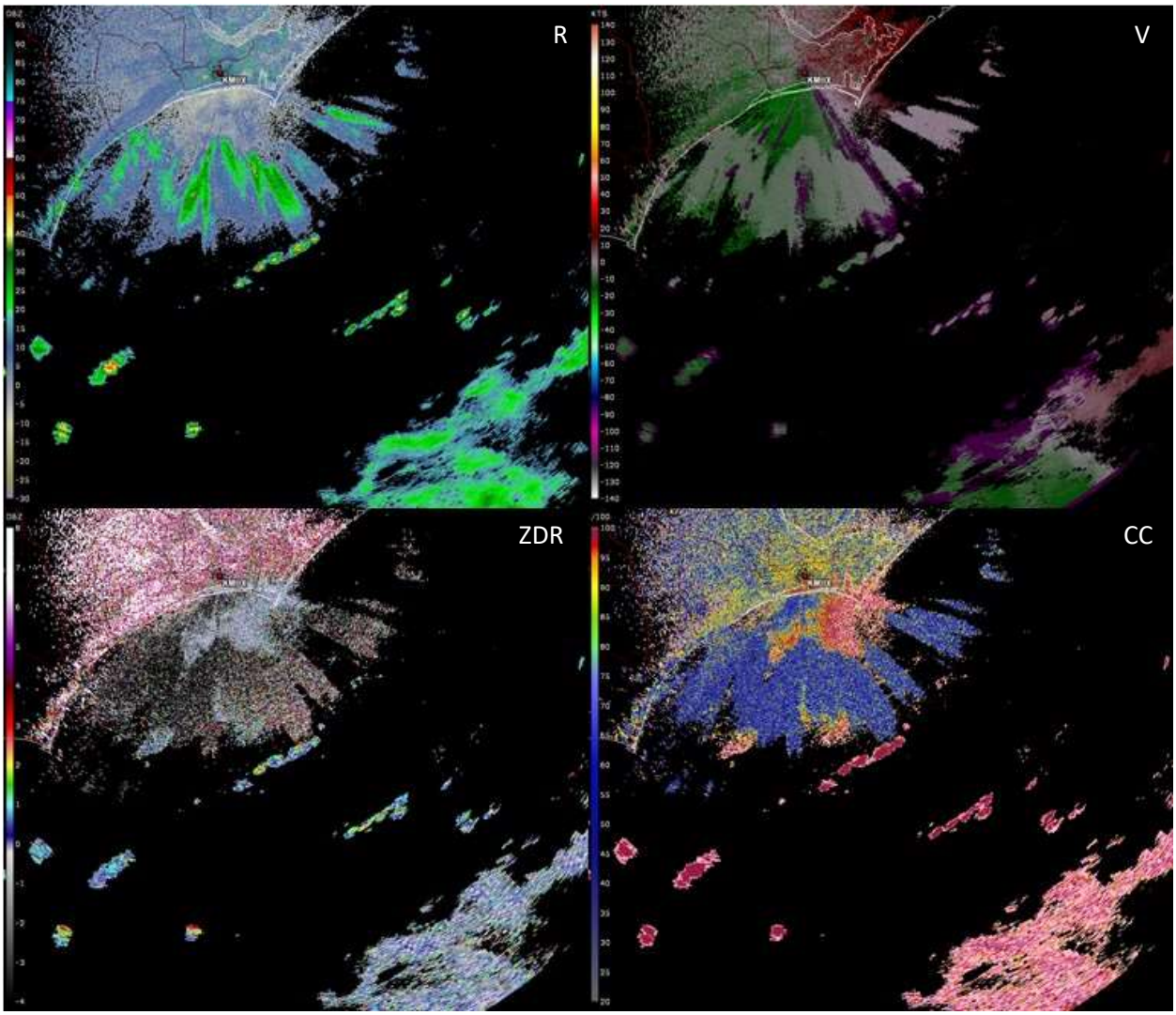

Sidelobe Contamination: Horizontal

Contamination from sidelobes can often be observed in radar data in areas of clutter, especially at sites with nearby mountains or elevated highways, in areas near storm cells, and during super refraction conditions. Proper clutter filtering can remove much of the sidelobe contamination in cases of stationary clutter. At the time of the event illustrated in the first 2-panel below, the site was running All Bins on Segment 1 and the static bypass map on all other segments. At 0.5 degrees, All Bins filtering was able to prevent the contamination from being displayed on the products while the other elevations were contaminated by sidelobes.

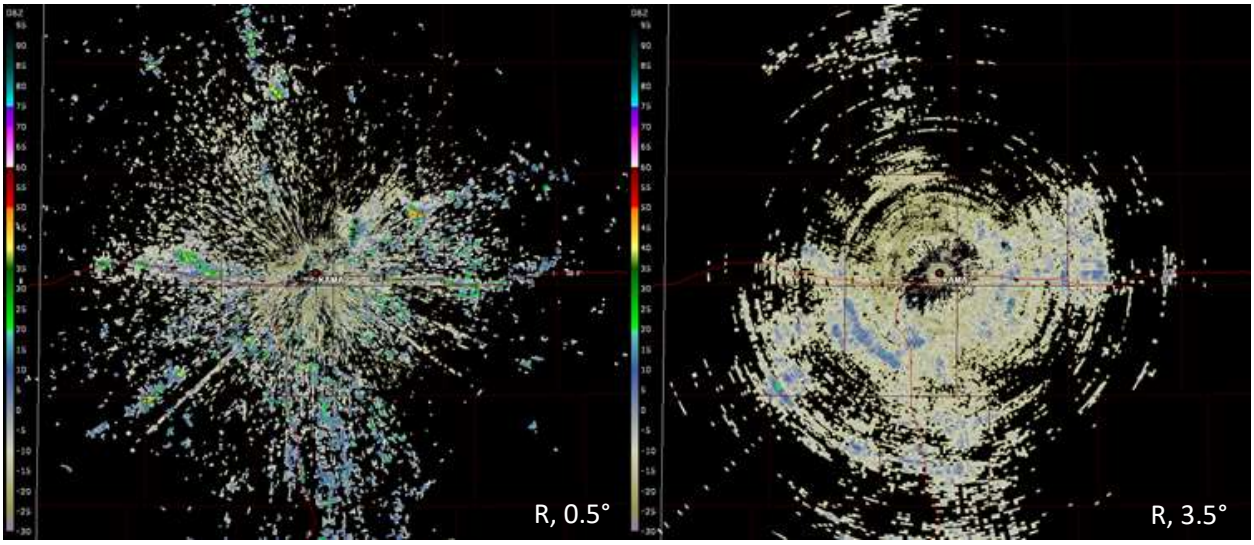

Sidelobes can contaminate data near strong storm cores, yielding a smeared appearance clockwise from the storm as observed in the 2-panel below. Note: The larger cone-shaped smear is due to a TBSS, which is discussed in a later section of this document.

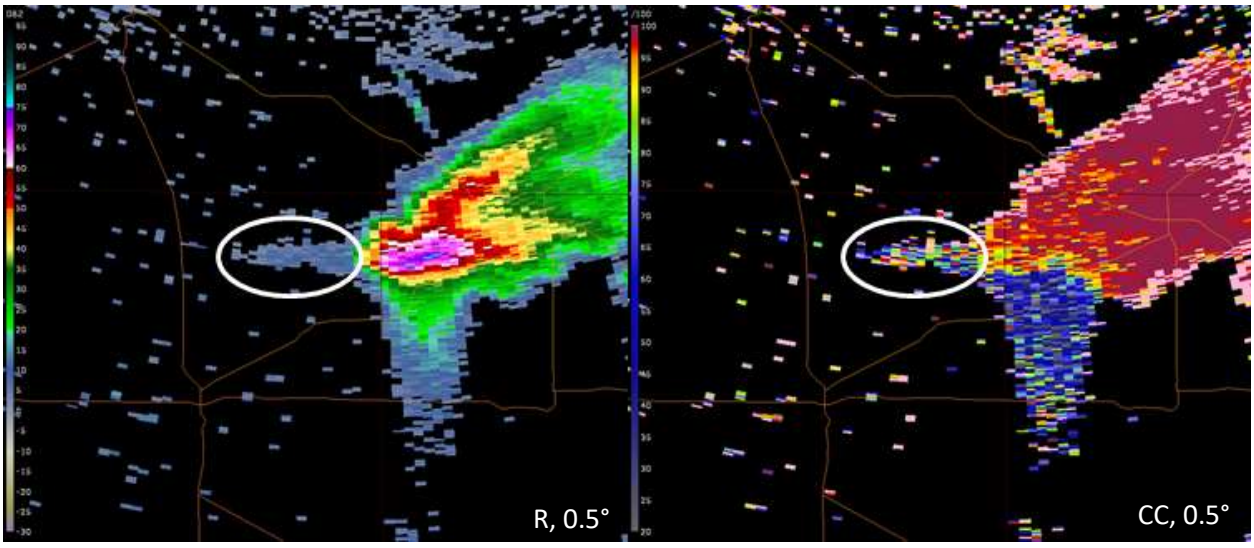

Sidelobe Contamination: Horizontal, continued

Sidelobe contamination can also manifest as small arcs as seen in the images below. Contamination from traffic along the highway can also be observed in the image.

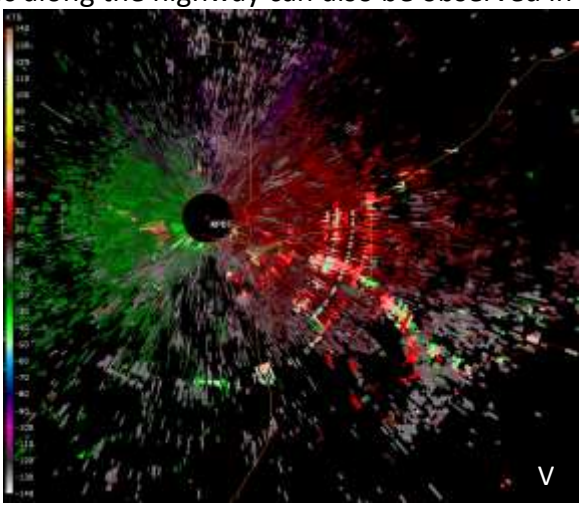

Sidelobe contamination has also been observed as arcs or even rings when trains are moving nearby to the radar. Examples of a train moving toward and away from a radar are shown below.

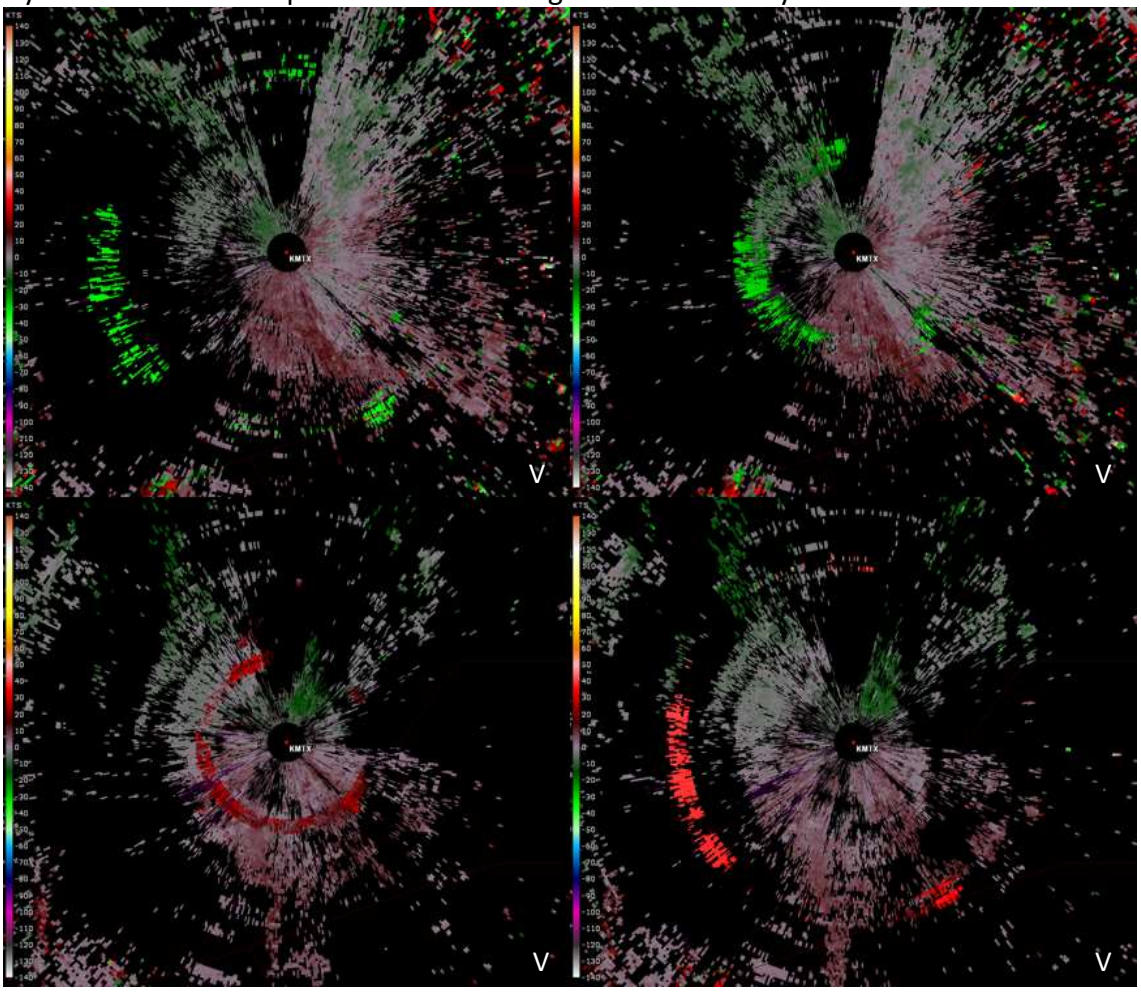

Sidelobe Contamination: Vertical

Generally weak returns are received from sidelobes and the returns we see on the display are typically dominated by the mainlobe. There are rare cases, like the one illustrated below, in which the sidelobes can contaminate the data when weak return is present in the mainlobe and strong return in the sidelobes. In this example, there is weak return at 0.5 degrees but a strong rotation signature is displayed in velocity. At 2.4 degrees, a high area of reflectivity is observed with strong velocities. In comparing the data from 0.5-degrees with the data from an upper tilt, it can be concluded that the velocity was contaminated by sidelobe contamination in the vertical.

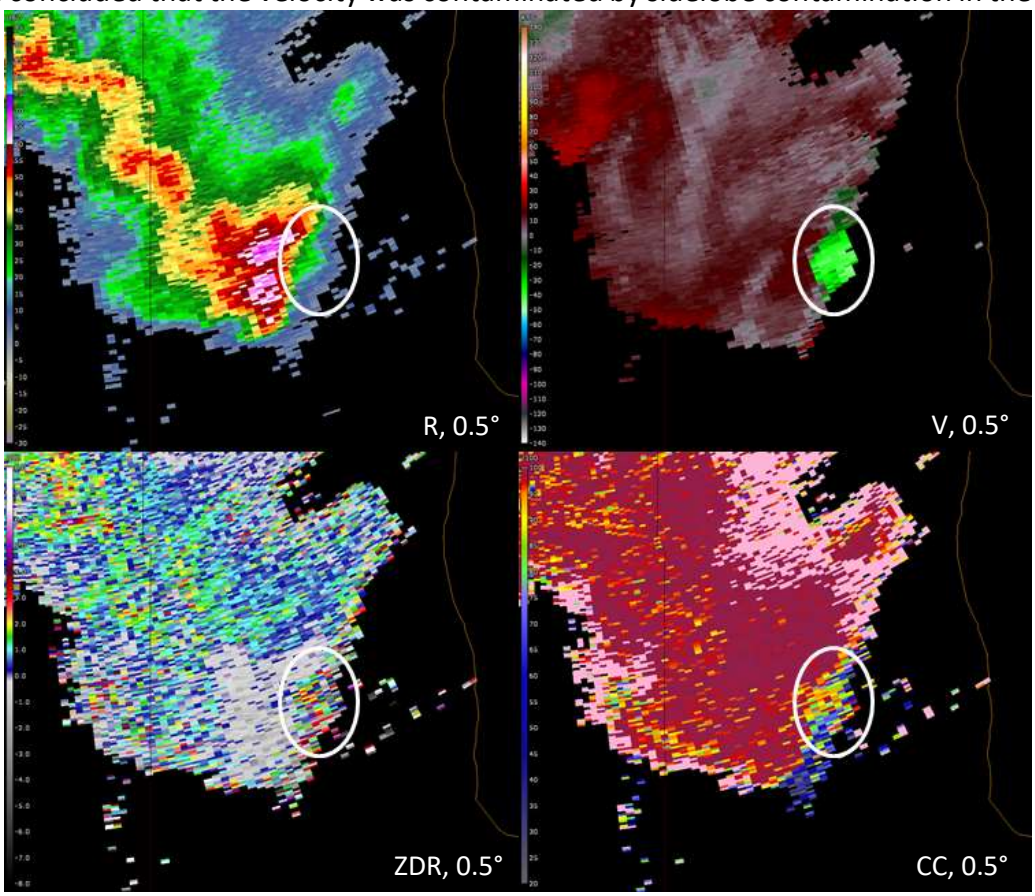

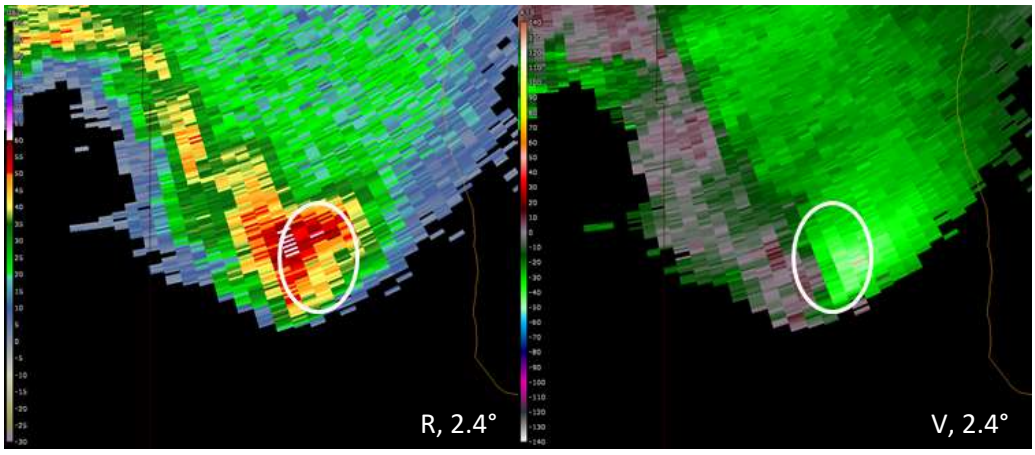

Sun Spikes

In Build 14, a superior noise estimation technique was fielded. One of the outcomes of estimating noise for every radial is that the sun spike is no longer visible. Or is it? Oftentimes a data void can be observed along the radial corresponding to the sunrise or sunset. Below is an example of one of these data voids due to the sun setting. The areas in which we see a void contain weak signal while the stronger signal from the convection is unchanged. When the noise exceeds the signal then a void can be observed.

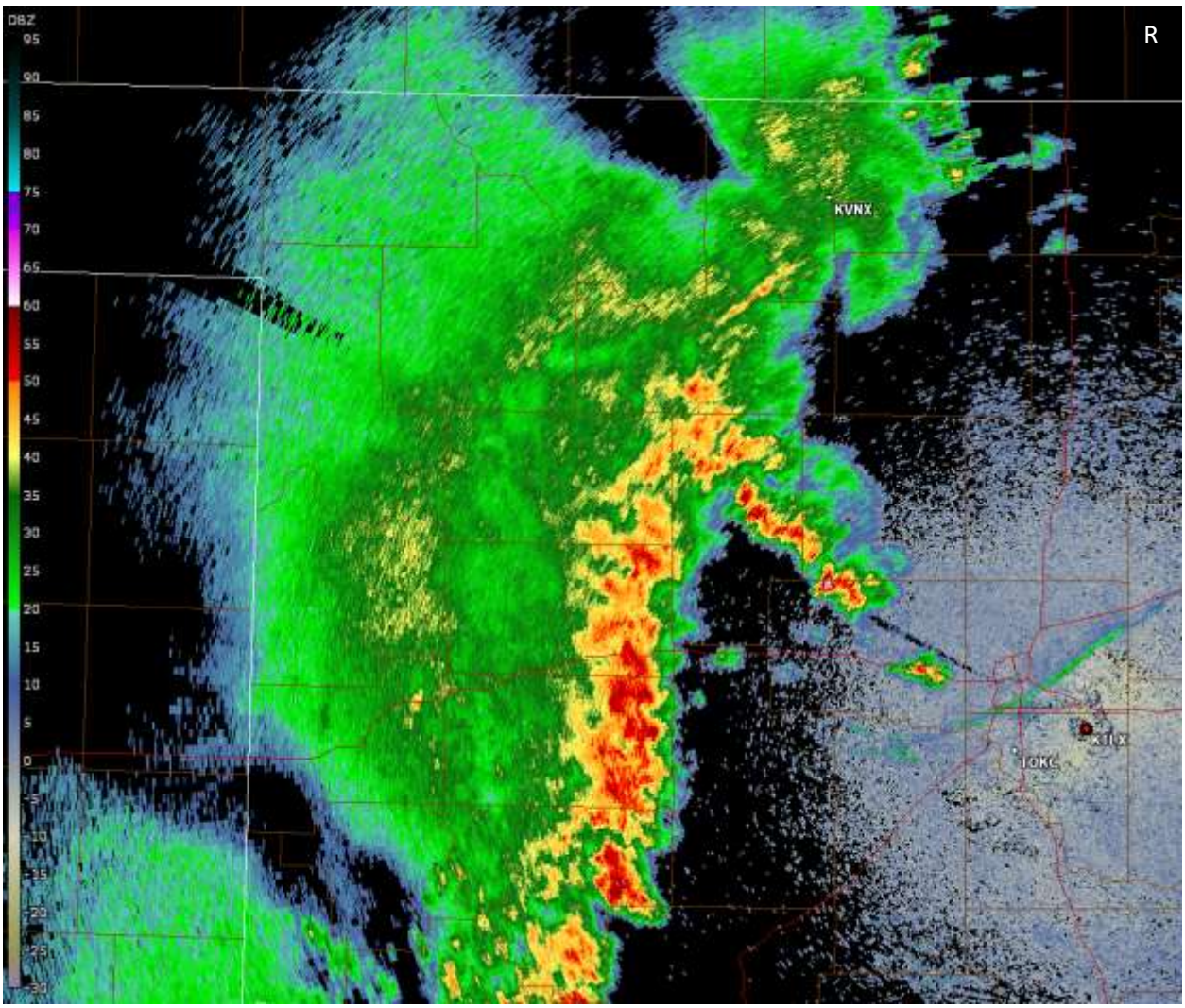

Start of Elevation Discontinuity

The start of elevation discontinuity can occasionally be observed in the data, especially when sufficient radar returns are present to allow observation of it. Often there is not a problem with the radar when this discontinuity is observed. This type of discontinuity can be due to slight elevation differences between the start and end of the elevation. Radar problems may exist if the observation is very frequent, there is a wedge of missing/incomplete data, or if the antenna continues to wobble throughout the cut and VCP. Note: If the discontinuity is also observed on the Doppler Cut of a Split Cut then the observation is not necessarily due to the start of elevation.

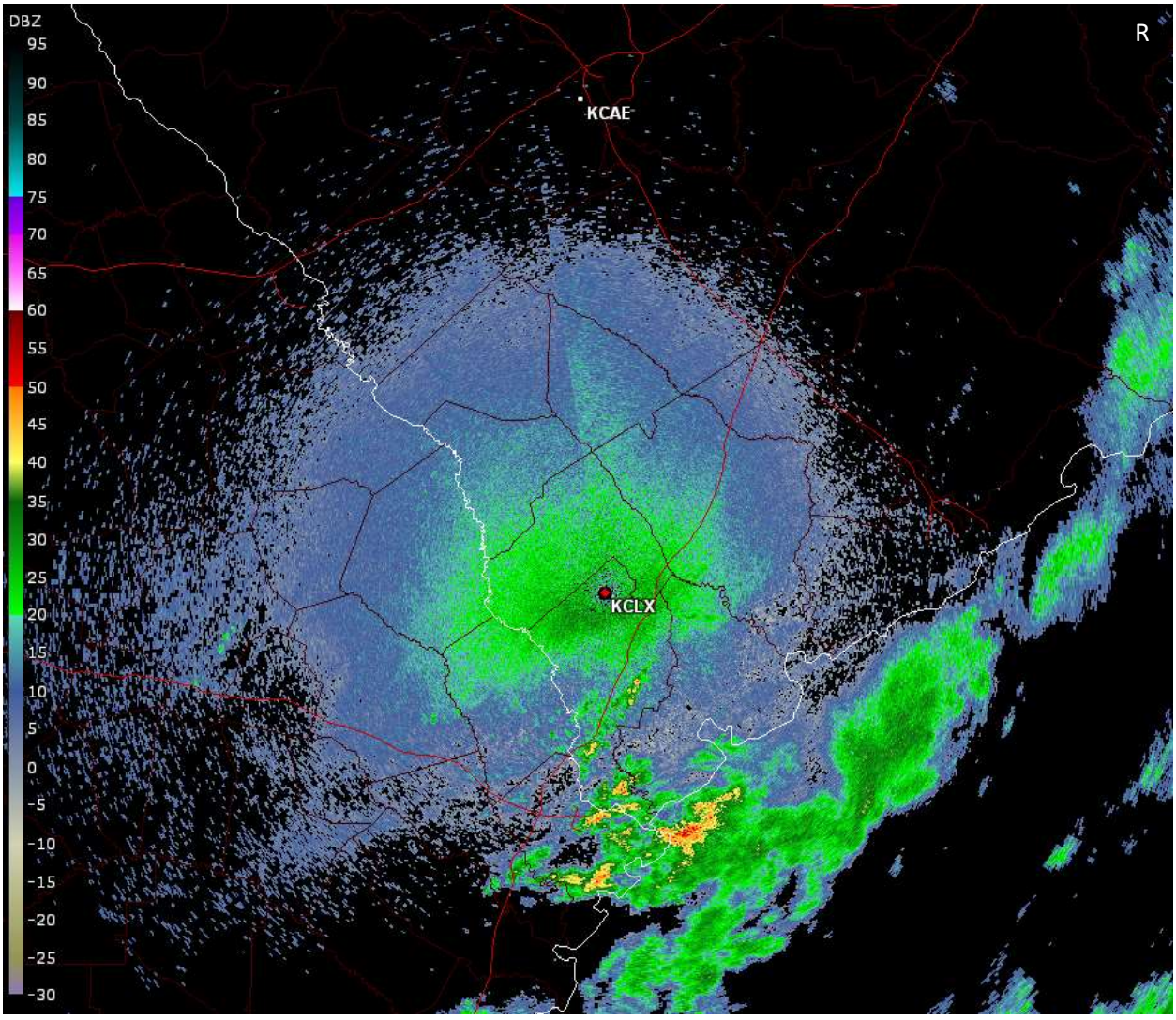

Stripes in SRM

Apparent stripes have been present in the SRM velocity product since its initialization. These discontinuities are an inherent result of mathematics used to compute storm relative motion from a velocity field. The stripes are seen more easily in a large, smooth stratiform field.

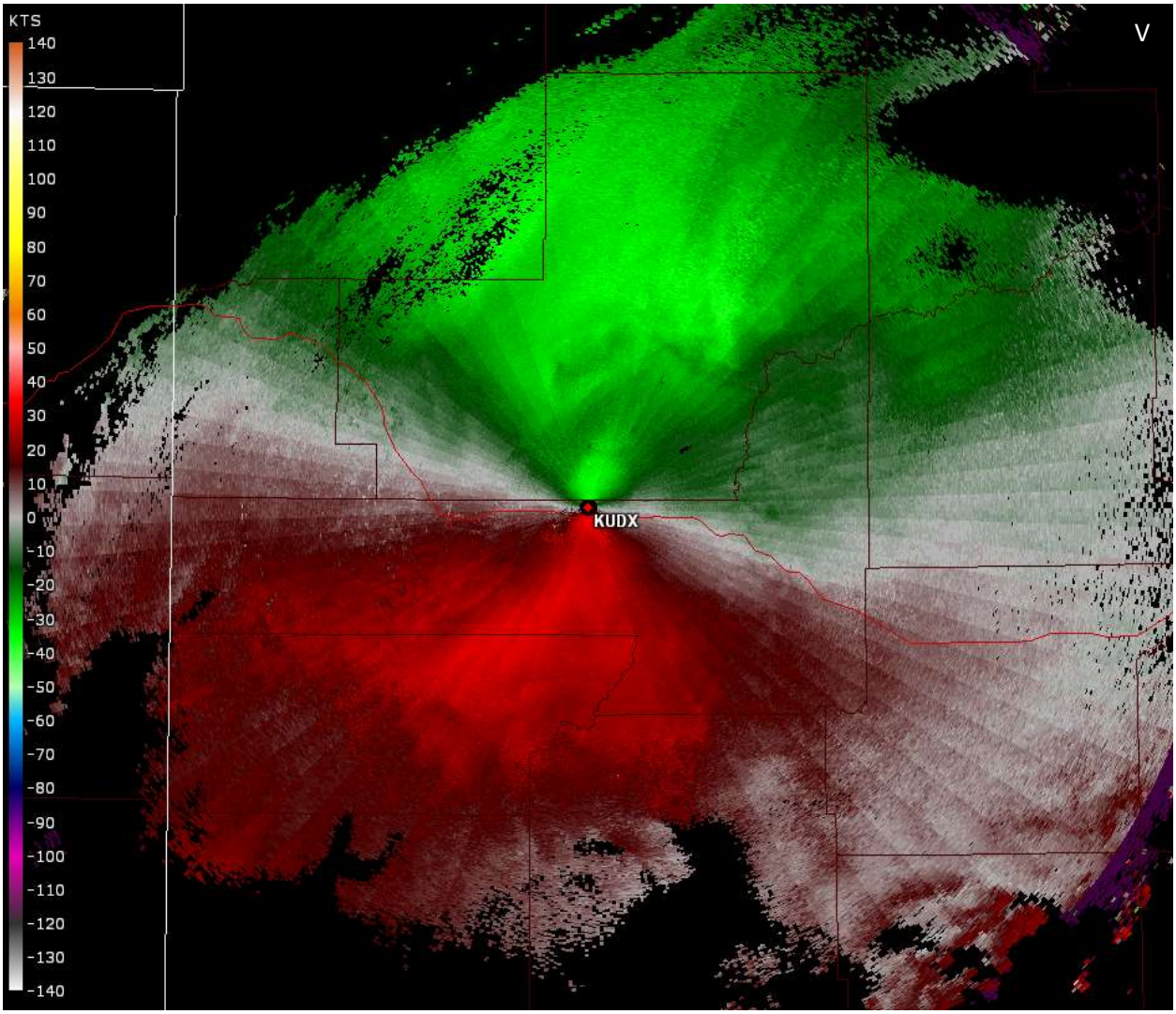

Terrain Spikes & Clutter Bursts

Terrain spikes have been observed in multiple VCPs but are often most apparent in VCPs 12 and 212. As the name implies, terrain spikes are radials of anomalous reflectivity that span across hills and mountains. These have been observed for several builds and regardless of the clutter map in place. In other words, terrain spikes continue to exist when forced filtering (i.e., all bins) is applied to the data. Occasionally, these same areas of clutter can increase or 'burst'. This anomaly is referred to as clutter bursts. Weather signal intensities do not increase during these bursts of clutter. No fix has been provided for these issues.

Terrain Spikes

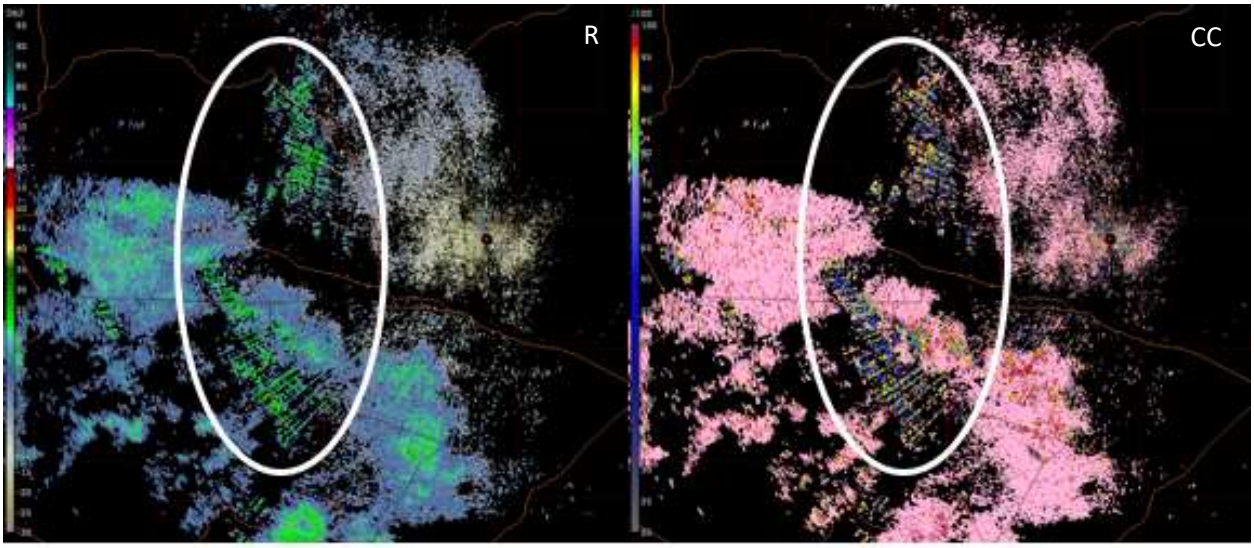

Clutter Burst

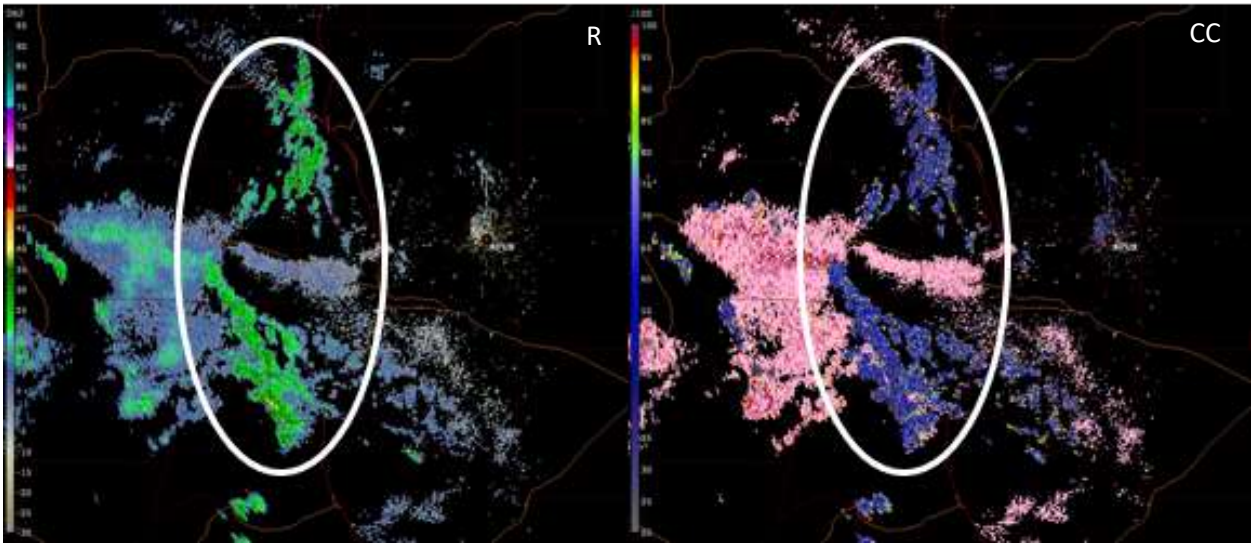

Three Body Scatter Spike

The phenomenon known as a Three Body Scatter Spike (TBSS) is the result of the radar beam passing through an area of high reflectivity. Within this area, the beam bounces off large hydrometeors, mostly large wet hail, which is subsequently deflected to the ground and back up into the storm before returning to the RDA. This produces a false radar echo that extends down radial from the storm. The spike can be seen not only in the reflectivity data but also in the CC data. The low CC values associated with this feature make it quite obvious.

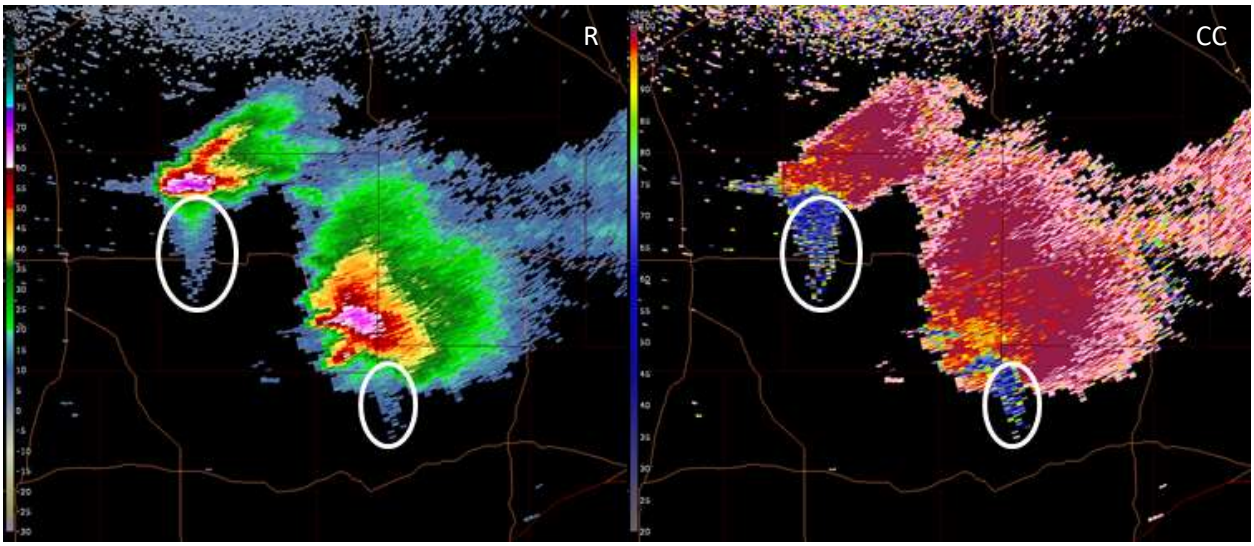

Velocity Dealiasing Errors: VCP 31

Due to a small Nyquist interval, VCP 31 is susceptible to velocity dealiasing errors. The errors in VCP 31 can have different visual characteristics, as shown in the examples below. Although 2D-VDA helps to mitigate the errors in VCP 31, errors can still occur. It should be noted that although VCP 31 is susceptible to velocity dealiasing errors it is a useful VCP, especially during drizzle or snow as it does have the best sensitivity of currently available VCPs.

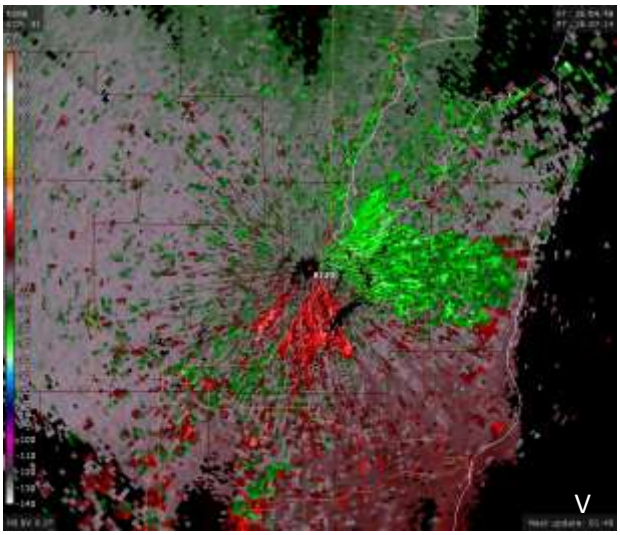

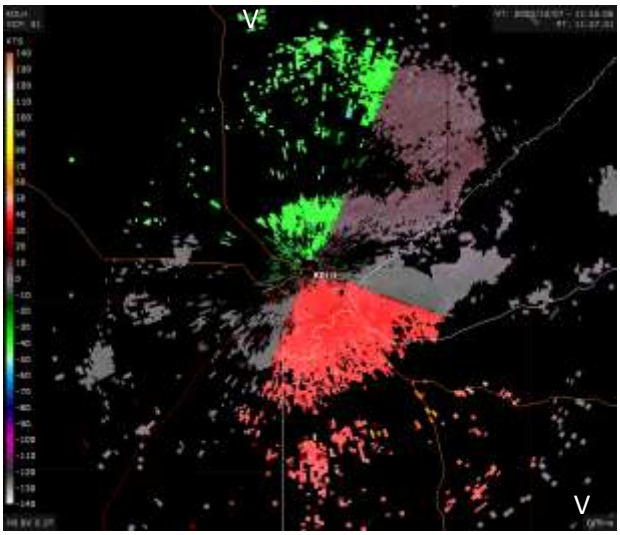

Velocity Dealiasing Errors

The following images illustrate examples of dealiasing errors. While superior to the Legacy VDA, the 2D-VDA continues to be refined in software upgrades when new dealiasing errors present themselves. Dealiasing errors can occur at far ranges or along strong shear gradients or outflow boundaries where it can be difficult to identify and properly dealias.

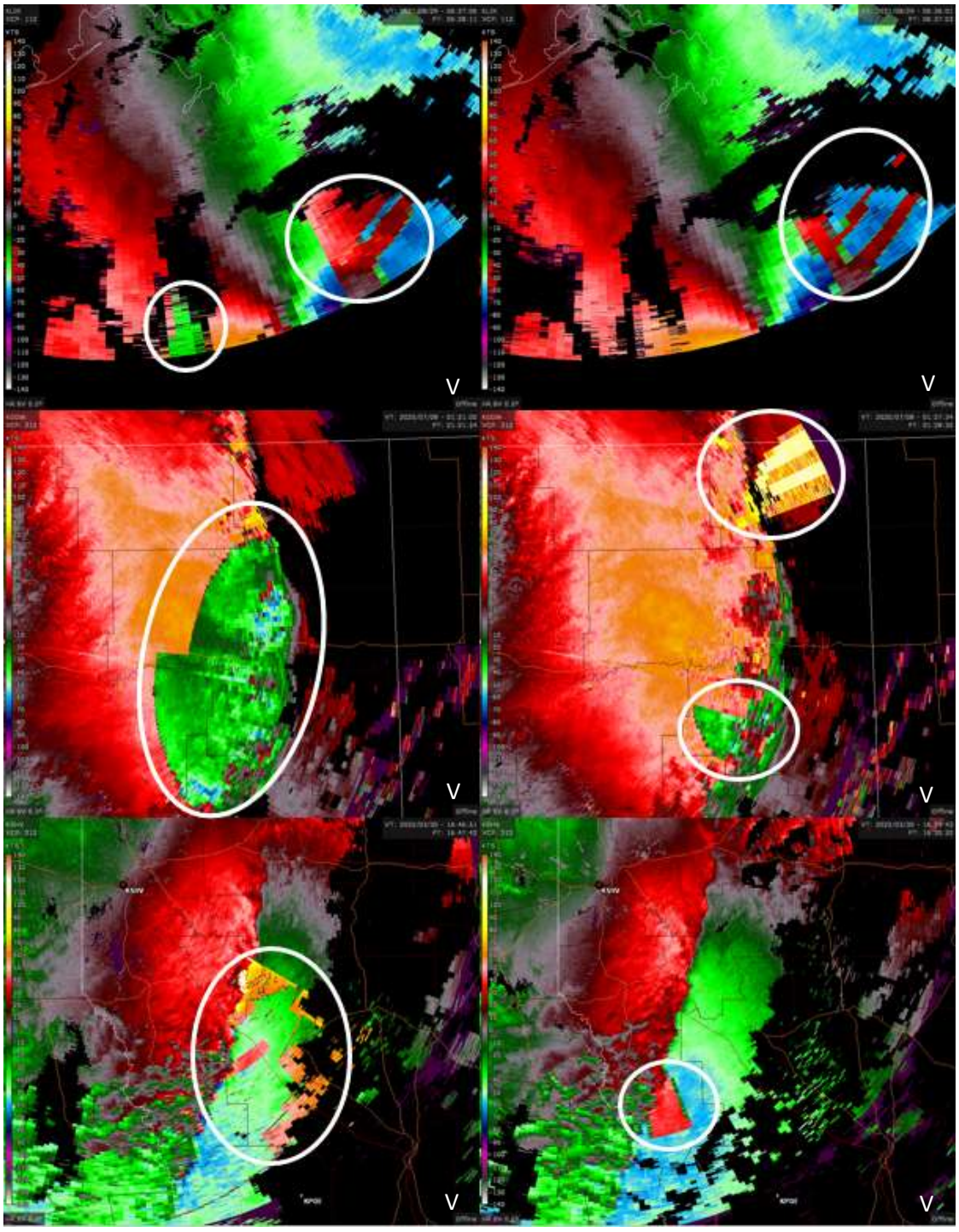

Wet Radome Effect

We are already familiar with the effect attenuation has on reflectivity. During an event, while precipitation is over the radome, there may be a couple of volumes in which the reflectivity estimates are lower than during the rest of the loop. The opposite observation may be seen in the ZDR estimates. It is theorized that as the precipitation forms rivulets along the side of the radome, the effect of attenuation is greater in the vertical than the horizontal causing a brief enhancement (or blossom) in the ZDR estimates. The examples below illustrate a wet radome effect with the images on the right showing the result of attenuation.

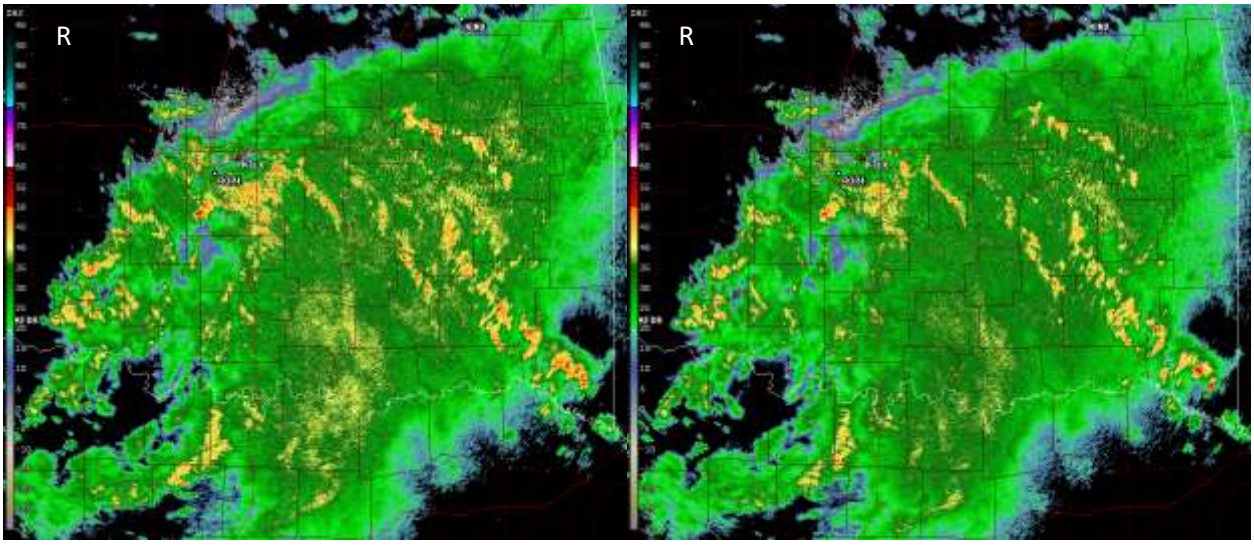

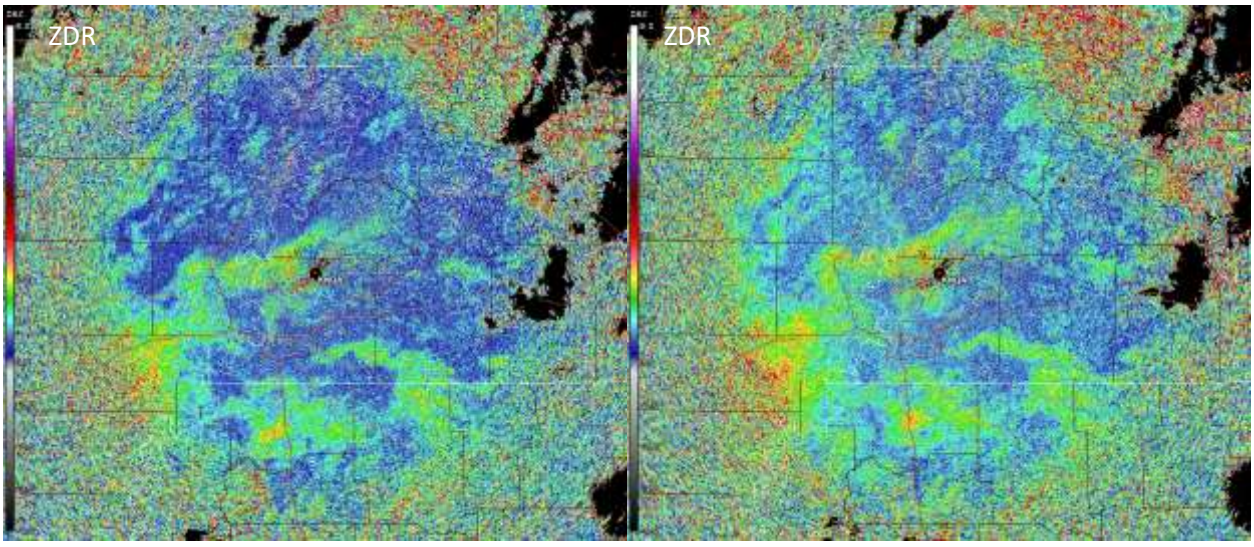

ZDR Wedges/Spikes

There are many reasons why we might see wedges (or spikes) of relatively higher, or lower, ZDR estimates. Some of these reasons are natural. There may be trees, cell towers, water towers, etc. that block the beam more in the vertical than the horizontal. This would lead to a wedge of increased ZDR estimates down range along the radial(s) from where the blockage exists. We have also observed depolarization, which often occurs in upper regions of thunderstorms and is the result of the reflected energy changing polarization. Lastly, differential attenuation occurs down radial of strong reflectivity cores and results in lower ZDR estimates down radial from the storm core.

Other examples of wedges of erroneous ZDR estimates have been a result of hardware issues, including loose cables. Some of the hardware issues have also resulted in rotating wedges of erroneous ZDR estimates or even wedges of no data. These wedges have shown higher and lower ZDR estimates and can be observed in both Level 2 and Level 3 data. Hardware-related issues, however, must be resolved by site personnel—WSR-88D Hotline assistance is available, as needed. Each ZDR wedge case is different and must be investigated in order to determine the cause.

Example of ZDR wedges due to partial beam blockages.

Example of ZDR wedges due to depolarization.

Example of ZDR wedges due to differential attenuation.

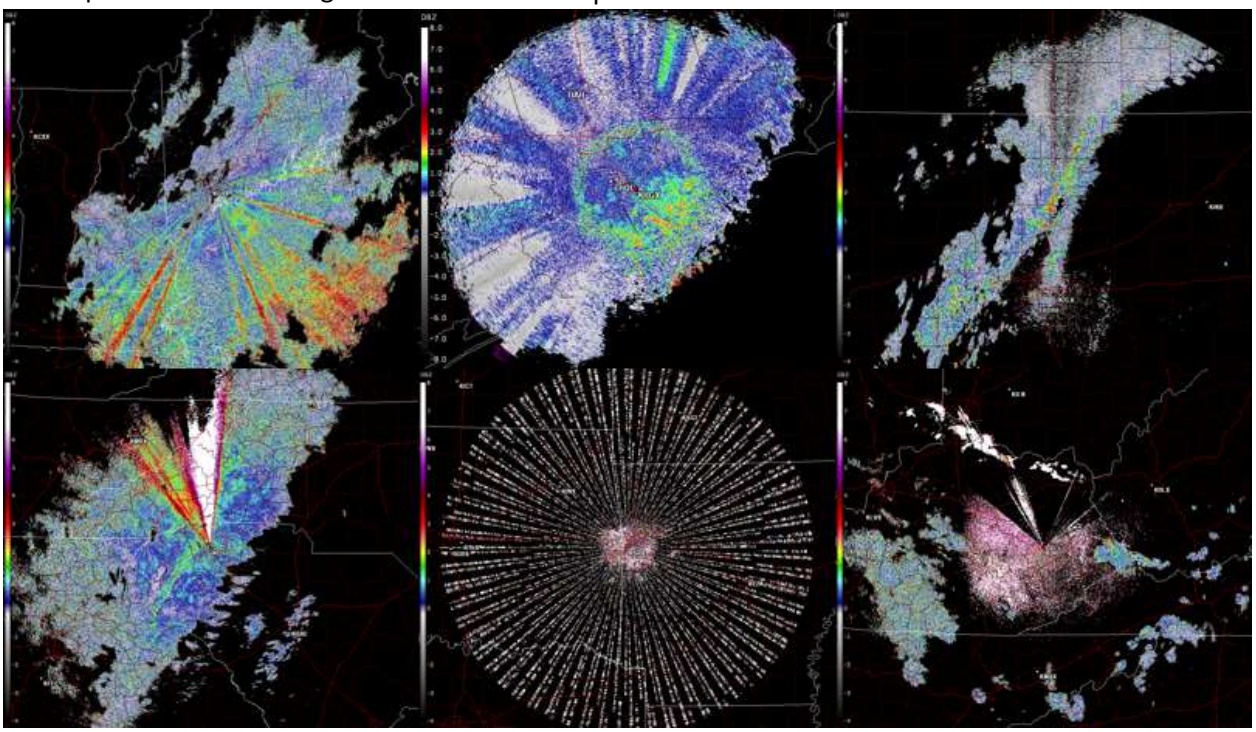

Example of ZDR wedges due to hardware issues. In this case, the wedge was resolved with replacement of the Azimuth Rotary Joint.

Example of ZDR spikes due to hardware issues.

Example of ZDR wedges due to hardware issues. In this case, the wedges were resolved by tightening the cables connecting one of the LNAs.

Past Topics:

Clutter Footprint

Formerly, CMD was not very efficient at identifying areas of weak clutter. Although all Dual-Pol variables are susceptible to the effects of missed clutter detections, Correlation Coefficient is particularly sensitive to clutter residue. The effects on the CC product have been termed "Clutter Footprint". Improvements were made to the CMD algorithm in RDA Build 18.2 which significantly reduces the Clutter Footprint issue in the Dual Pol variables. Note that this change does not affect the legacy base data (i.e., R, V, and W). Below is an example of the same volume of data with and without the improvements deployed in RDA Build 18.2.

CC before the RDA Build 18.2 Improvements

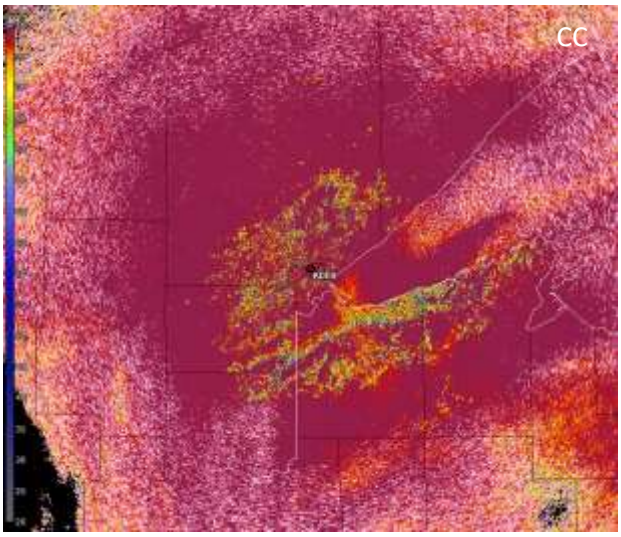

CC with the RDA Build 18.2 Improvements

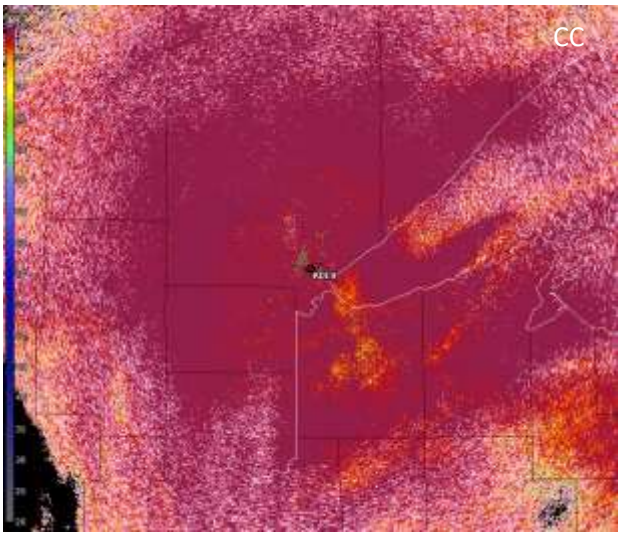

Corresponding reflectivity image

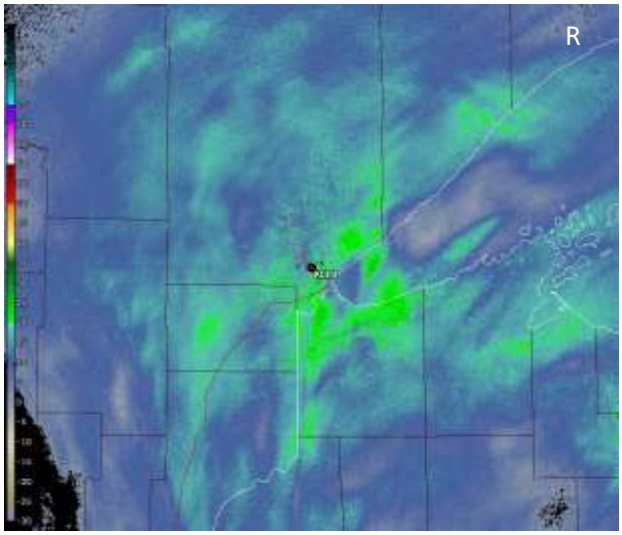

PHI Initial Target Value

Prior to RDA Build 14.0, the initial target value for PHI estimates was 25 degrees. Starting with RDA Build 14.0, however, the target value changed to 60 degrees. The goal of this change is to mitigate how often the ISDP calibration needs to be completed. Tweaks to hardware (i.e., cables) and changes in ambient temperature can result in shifts or drifts in the initial value. Repeated drifts can result in the PHI Wrapping issue discussed in this document. A new color table has been developed for the new target so the color of 60 degrees is blue. If using the original color table for PHI (with Build 14) then one would expect dark green. Below is an example of the same volume of data processed from RDA Build 14. The image on the left is displayed with the original color table while the image on the right is displayed with the adjusted table so that we see blue, as accustomed. Note: The initial PHI value is estimated at the edge of precipitation nearest the radar.

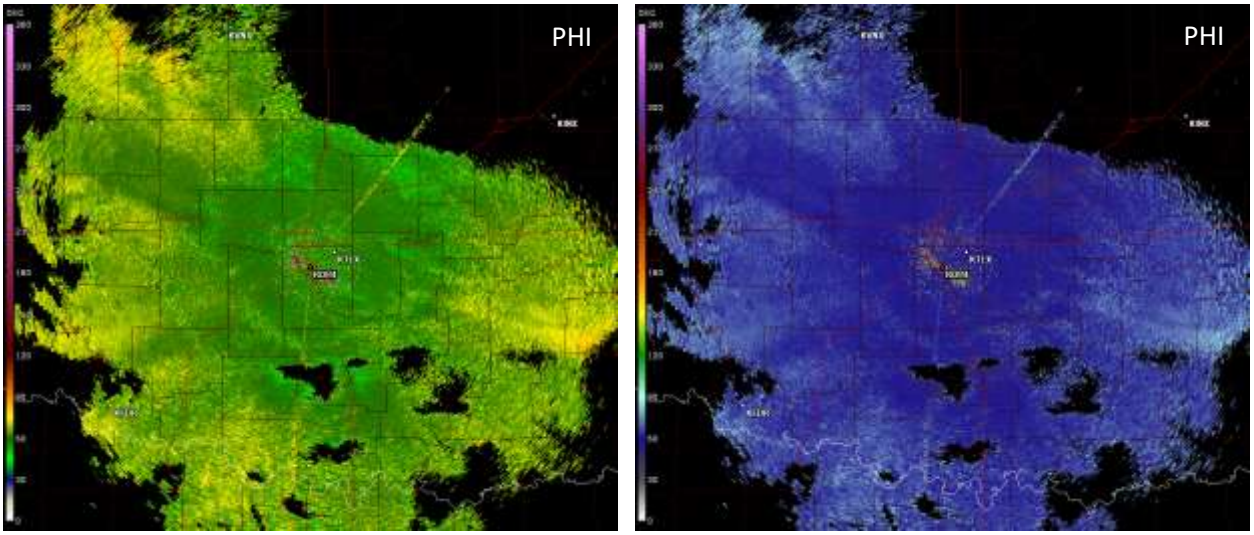

Radial Spikes of Zero Knots in Spectrum Width

Observations of radially-oriented spikes of zero knots in Spectrum Width products were documented in previous software builds. These spikes were observed ***only*** in Batch Cuts of VCP 32 when PRF 8 was active.

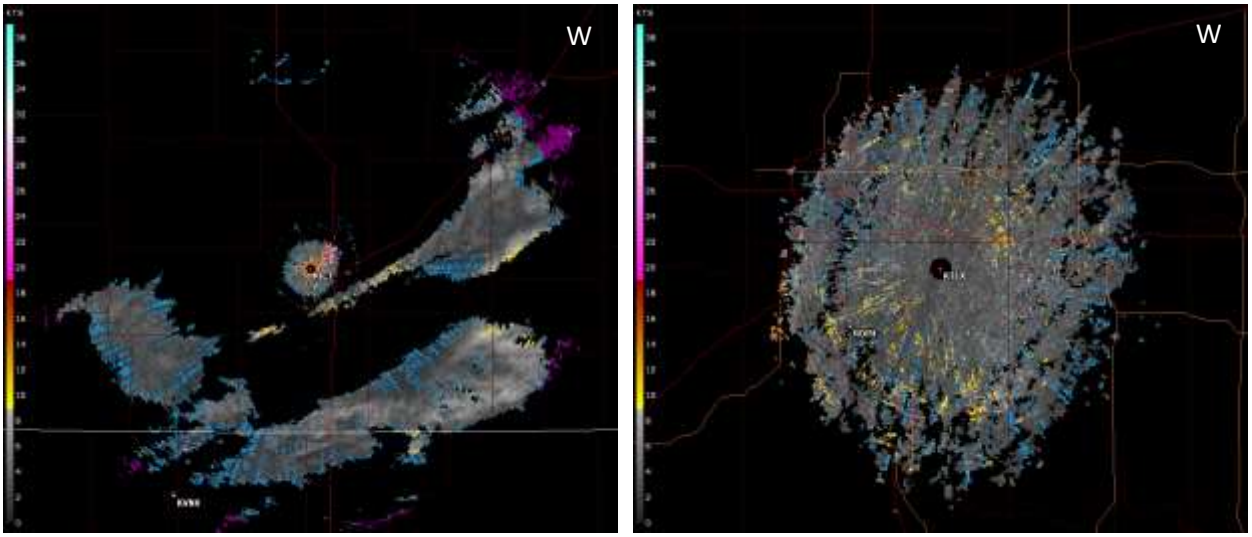

Shimmy

The "shimmy" was discovered when Super Resolution data became available; although, the problem had existed for numerous builds. The "shimmy" was an apparent shift in the radar data which could be observed when switching from a clear air VCP to a precipitation VCP and vice versa. Examples from the field have been documented in the WSR-88D Field Support Hotline. The cause of this issue was due to latency between the DCU and the RCP8/RVP8 and was fixed in Builds 10.3 and 11. As a side note, the DCU became obsolete with the introduction of the Radar Signal Processor in Build 17.

SZ-2 in Manual PRF Bug

In Build 16.0, SZ-2 PRF selection was introduced. This change also introduced a bug. For manual PRF selection, the RPG HCI failed to change the scan rate for SZ-2 cut when the operator changed the PRF value. When this occurred, the RPG received numerous "Number of Recomb Rads in Cut > 400 → Forced End of El/Vol" messages, which often resulted in wedges of "no data" on many Level 3 products. This issue was fixed in Build 18.

Acronyms

2D-VDA	Two-Dimensional Velocity Dealiasing Algorithm
AWIPS	Advance Weather Interactive Processing System
CC	Correlation Coefficient
CMD	Clutter Mitigation Decision
dBZ	Decibel Relative to Reflectivity
DHR	Digital Hybrid Reflectivity
DoD	Department of Defense
DSP	PPS Digital Storm Total Precipitation
DSA	QPE Digital Storm Total Accumulation
FAA	Federal Aviation Administration
GMAP	Gaussian Model Adaptive Processing
HCA	Hydrometeor Classification Algorithm
HC	Hydrometeor Classification
HHC	Hybrid Hydrometeor Classification
HSR	Hybrid Scan Reflectivity
ISDP	Initial System Differential Phase
KDP	Specific Differential Phase
LNA	Low Noise Amplifier
NBF	Non-Uniform Beam Filling
PHI	Differential Phase
PPS	Precipitation Processing Subsystem
PRF	Pulse Repetition Frequency
QPE	Quantitative Precipitation Estimation
R	Reflectivity
R&R	Removal and Replacement
RDA	Radar Data Acquisition
ROC	Radar Operations Center
RPG	Radar Product Generator
SRM	Storm Relative Motion
STA	QPE Storm Total Accumulation
SW or W	Spectrum Width
SZ-2	Sachidananda-Zrnić Phase Coding
TBSS	Three Body Scatter Spike
UTC	Coordinated Universal Time
V	Velocity
VCP	Volume Coverage Pattern
VDA	Velocity Dealiasing Algorithm
WSR-88D	Weather Surveillance Radar-1988 Doppler
ZDR	Differential Reflectivity